# Controls on syn-kinematic sedimentation in an asymmetrical extensional basin, Sorbas basin SE-Spain

Msc Thesis: Louis van Noorden

Student nr. 3507912

Utrecht University, 2014

## Abstract

Asymmetrical extensional basins are often associated with large-scale footwall exhumation. The sediment supply from this footwall is controlled by tectonics controlling relief (slope) and rejuvenating the source area as well as climate, controlling precipitation and weathering rates. Contemporaneously, tectonics and climate control base-level fluctuations in the hanging-wall. Thus both supply and accommodation-space are expected to be strongly controlled by tectonics and/or climate during active extension. We aim to improve the understanding of how this balance between tectonics and climate affects the distribution of facies in the basin and how it evolves trough time during active extension.

The Sorbas basin (SE Spain) is such a basin located in the hangingwall of an extensional detachment with a marked asymmetric architecture. In order to study the link between controls, high resolution sequence stratigraphy and structural analysis is performed on the syn-kinematic Tortonian deep-water sequence in order to capture the cycles of different scales.

Large scale (multiple 100s of meters) non-cyclical facies changes were mainly influenced by changes in the source area induced by tectonics and changes in the slope gradient. Smaller scale (20-150m) changes in facies show a tectonic signature in the first part of the basin fill while toward the end of the Tortonian climate likely controlled the sediment supply to the basin. The smallest scale cycles (meter scale) that could be distinguished were observed along syn-depositional faults likely relate to activity on the main fault.

## 1. Introduction

The main controls on the sedimentary basin fill are tectonics and climate, both able to influence the supply of sediment and the accommodation space in a sedimentary basin (*e.g. Schlager 1993*). These controls are often expressed in cyclical sedimentary patterns of different facies in the basin fill (*e.g. De Boer and Smith 1994, Pereira and Alves 2012*). The controls act on different timescales superimposing higher frequency cycles on lower frequency cycles (e.g. *Catuneanu 2006*). Sequence stratigraphy is used to link the different facies in the cyclical patterns to transgression and regression, distinguish between different hierarchies and ultimately attribute the cycles to external controls (*e.g. Martins-Neto 2010, Mitchum & van Wagoner 1991*).

Basins in the hangingwall of extensional detachments are often associated with large scale-footwall exhumation (e.g. *Wernicke 1988*). Their asymmetric geometry leads to a significant difference in the hangingwall- (low angle) and footwallslope (high angle). The sediment supply from the footwall is controlled by tectonics controlling relief(slope) and rejuvenating the source area as well as climate, controlling precipitation and weathering rates. At the same time, tectonics and climate control base-level fluctuations in the hanging-wall (*e.g. Gawthorpe 1994*). Thus both supply and accommodation-space are expected to be strongly controlled by tectonics and/or climate during active extension. We aim to acquire a better understanding of the effects of this interplay between tectonic controls and climate in these types of basins during active extension, such as how it affects the distribution of facies in the basin and how it evolves trough time.

The Sorbas basin (SE Spain) is such a basin located in the hanging wall of an extensional detachment (*e.g. the Alhamilla detachment, Martinez-Martinez and Azanon 1997*) with a marked asymmetric architecture (*do Couto et al. 2014*). The extensional detachments forming the border to the south of the basin controls the subsidence of the basin as well as the exhumation of a metamorphic complex in the footwall. The Tortonian deep-water sequence was deposited during active extension (*e.g. do Couto et al. 2014*) and is well exposed making it suited for high resolution logging. In order to study the link between controls, high resolution sequence stratigraphy and structural analysis is performed in order to capture the cycles of different scales and an attempt is made to correlate these cycles to internal or external controls.

## 2. Geological setting

The Sorbas basin is part of a series of Neogene intra-montane basins in the Betic Cordillera, located in the South East of Spain (fig. 1). The Betic basins are relatively short lived (active for less than ~13 Myr) and are marked by rapid subsidence mainly during Tortonian times (*Rodríguez-Fernández 2011*). The origin of the subsidence in the basins has been attributed to strike-slip tectonics in the past (*e.g. Montenat & Ott d'Eestevou 1999*). More recently however strike–slip tectonics are viewed as a late-stage overprint and the nature of Betic basin formation is viewed as purely extensional (*e.g. Meijninger and Vissers 2006, Rodríguez-Fernández and Sanz de Galdeano 2006*).

### 2.1 Tectonics, Basin and Basement formation

The Sorbas Basin is bound by the Sierra de los Filabres in the North and the Sierra Alhamilla in the South (fig. 1). These sierras contain two tectonic units comprising different metamorphic units, the Nevado-Filabride complex and the overlying Alpujarride complex. These units form the basement to the Sorbas Basin. These metamorphic complexes were rapidly exhumed during the early Miocene (*e.g. Johnson 1997; Platt 2005; Vazquez 2011*) in the footwall of asymmetrical low-angle detachments formed under ~E-W extension (*e.g. Augier 2005*). By the early Tortonian, extension occurred in the brittle domain forming the half-graben structures of the basin (*Augier 2005*; *Augier et. al 2013*). The direction of extension had rotated and was N-S to NNW-SSE during this interval (*Augier et. al 2013*). Subsequently the Sorbas Basin was subjected to a compressional regime expressed along the basin margin where high angle reverse faults have thrust metamorphic basement over the sedimentary basin fill (*e.g. the North Alhamilla Reverse Fault (NARF); see fig. 1; fig.5; do Couto 2014*) as well as in intrabasinal high angle reverse faults deforming Tortonian sediments (*e.g. Cantona faultzone (CFZ); fig. 2, fig.5; Haughton 2001*).

In the study area, the Nevado-Filabride (NF) complex is generally divided into two units. The lower unit contains dark colored medium grade graphite schists. The upper part contains mainly tourmaline gneiss, marbles and graphite schist (*Martinez-Martinez & Azanon 1997*).

Two units have also been distinguished in the Alpujarride complex. The Lower unit contains calcite dolomite marbles, lights schists and phyllites and graphite schist (*Martinez-Martinez & Azanon 1997)*. The upper part contains characteristic purple Permo –Triassic phyllite, quartzite and a thick sequence of Triassic dolomitized carbonate platform sediments (*Vissers 1995; Martinez-Martinez & Azanon 1997*). The Alpujarride rocks are outcropping in the limbs of the open anticline of the Sierra Alhamilla along its northern and southern flank but have been eroded in the core where NF complex is exposed (fig.1) Also in the Sierra de los Filabres the Alpujarride complex has been largely eroded (fig.1). These distinct metamorphic complexes in combination with the exhumation history of the sierras are useful for determining the source area of the sedimentary basin-fill (see Ch. 2.4).

### 2.2 Tortonian – Messinian Basinfill

Opening of the Sorbas basin took place with the onset of coarse fluvial to shallow marine conglomerates which can be found outcropping in the east of the basin (fig. 2). The deposits are believed to be of Latest Serravallian to Early Tortonian age (*Weijermars 1985*). This was followed by a rapid transgression that led to the deposition of a deep-water turbiditic system. On the northern slope south of Sierra de los Filabres coral reefs on platforms and fan deltas were located (*Braga 2003 and references therein*). During the latest Tortonian platform carbonates (Azagador formation) were deposited in the basin during rapid progradation, its base being locally dated at 7.5Ma (*Puga-Bernabéu et al. 2007; de Winter and Hartman, unpublished*). This unit is outcropping along an East-West trending cuesta throughout the basin (fig.2).

The shallow marine carbonates grade upward and laterally into marls (*Martín & Braga 1994, Sánchez-Almazo 2001*). These pelagic marls (Abad formation) are deposited in a thick sequence on top of the carbonate platform deposits (fig.2 & 4). The Abad formation is generally divided into an upper and lower part marked by changes in lithology and fauna, a change that occurred at 6.70 Ma (*Krijgsman et al. 2001*). The marls of the Lower Abad formation were deposited during a large scale transgression and rapid deepening of the basin (*e.g. Baggley 2000*) which started near the Tortonian-Messinian boundary (7.24 Ma*, Hilgen et al 1995; Krijgsman et al. 2001*). Contemporaneously, bio-herms were deposited on the basin margins (*Riding 1991, Martín and Braga 1997*). The upper Abad unit is associated with progressive shallowing and restriction of the basin (*e.g. Sierro et. al. 1999; Baggley 2000*). Laterally equivalent to the upper Abad are Messinian fringing reefs which were deposited against the bioherms separated by a minor unconformity (*Martín and Braga 1996, Riding 2000*). Finally during the Late Messinian, the Messinian Salinity Crisis caused massive deposition of evaporitic gypsum in the center of the basin (Yesares Formation).

The Tortonian sequence in the Sorbas basin has been inverted after its deposition, resulting in transpressional folding and faulting with deformation becoming more intense towards the southern boundary where the stratigraphy is locally overturned (fig. 5). The age of the inversion event is still unclear in existing studies but the onset must be older than Messinian as the fringing reefs of this age are deposited unconformably and are found presently at low inclinations over the steeply dipping Tortonian deep-water deposits in the south of the basin (*Martin and Braga 1990, Weijermars 1985*). This inversion also has its implications for the most proximal deposits along the southern border which have been eroded subsequently (fig. 5).

### 2.3 Existing sedimentary models for the Tortonian basin-fill

*Early Tortonian*

The sedimentary model of Haughton (1994) envisages that gravity driven flows sourced from the north are distributed along the narrow, trough-shaped depocenter. Important aspects of this distribution are the deflection and ponding of the flows. Flows are running from the northern slope up the southern slope of the Sierra Alhamilla where they are deflected and run backwards off this slope reworking previous deposited sediments (possibly from the same flow). This process can explain the complex grading in the deposits of the gravity flows (*Haughton 1994*). In addition because the silts and clays cannot escape the confined setting (ponding), relatively large mudcaps are deposited.

*Late Tortonian*

The general consensus is to attribute the transition of the deep-water sequence to the Latest Tortoninan shallow marine deposits to an inversion of the basin (e.g. *Weijermars 1985; Braga 1996; do Couto 2014*). This is mainly inferred from the observation that the turbidites are dipping at higher inclinations than the shallow marine carbonates on top which is consequently interpreted as an angular erosional unconformity. In this research we contest this view and argue that an inversion is not necessary to explain the transition from deep-water to shallow marine.

### 2.4 Source areas and their exhumation

The geometry of the source area and its paleogeography is an important variable that is changing significantly throughout the evolution of the Sorbas Basin. There are two possible source areas for the Sorbas basin. A source area in the footwall which is the Sierra Alhamilla/Cabrera and one associated with the hanging wall, the Sierra the los Filabres (fig. 1). The Nevado-Filabride complex in the Sierra de los Filabres, bounding the north of the basin, reached near-surface temperatures as early as 12-13 Ma in the area of the Sorbas basin based on apatite FT analysis (*Johnson et al 1997, Vazquez et al. 2011*). This is in concordance with the timing of the fluvial to marine conglomerates (fig. 2) found in the oldest parts of the basin (*Weijermars 1985*).

Based on apatite fission tracks the Alpujarride complex of the Sierra Alhamilla and the underlying Nevado-Filabride complex did not reach near surface temperatures until 8-10Ma and 6 Ma respectively (*Platt et al 2005*), indicating a later timing of exhumation than the sierra de Los Filabres. Current directions and the geometry of sediment bodies from the neighboring Tabernas basin do indicate that the Alhamilla was a submarine swell forming the basin boundary in the south (*Haughton 1994, 2000*). This means that the Sierra Alhamilla was probably not a source area during most of the Tortonian but it could have become a source area during the upper Tortonian.

## 3. Methods and Approach

The combined kinematic and sedimentological analysis of the southern part of the Sorbas basin was performed by the means of a high-resolution profile, whose trace was chosen to maximize the continuity and lateral correlation between outcrops (fig. 3). The ~2 km long profile extends from the base of the Latest Tortonian carbonate-platform unit until the present southern basin margin, where a large transpressional fault zone can be observed (fig. 3). Because the strata were subsequently tilted between 40 and 80 degrees after (syn-kinematic) deposition (fig. 3 & 5), a lithostratigraphic column of the basin can be obtained for most of the Tortonian evolution of the Sorbas basin. The field mapping involved measuring the kinematic characteristics of various phases of deformation and a sedimentological/sequential stratigraphic analysis of the observed deposition.

The kinematic mapping involved measurements of fault kinematics, including fault planes and kinematic indicators, such as slickensides, Riedel fractures, drag-folds and conjugate faults. A few folds were measured in the field by fold axial planes and hinges. In particular important was the observation of syn-depositional versus post-depositional character of faulting and their correlation along the stratigraphy of the observed profile. Because a significant number of faults were tilted after their formation, we used bedding measurements to analyze and restore them to their original spatial position. All this allowed the definition of the stratigraphic moments of deformation and their evolution in time.

The aim of the sequence stratigraphic and sedimentological analysis was to correlate the kinematic deformation with the response of sedimentation in the basin. This was achieved by mapping facies units that were subsequently grouped in facies associations and the definition of sedimentological environments. The facies units defined in the high resolution profile are the lithological types ranging

from 15cm to 2m (see Appendix B). In the turbiditic environment that dominates the sedimentation in the studied profile, these are formed in response to one individual sediment flow (although more complex types are recognized) marked by an overall fining upward trend from coarsegrained turbiditic/debris flows to more pelagic sedimentation. Each facies unit (or type) has its characteristic layer size, grainsize, lithology and internal structures which show similar properties (Appendix B).

These types are grouped into facies groups (or parasequences) on the basis of similar properties and process of deposition (e.g. debrite vs. turbidite or pelagic sedimentation). These lithofacies groups are genetically associated with different depositional systems. These groups are interpreted in relationship with neighboring units in the high resolution section (Appendix A) and are consequently grouped as facies associations (e.g. *Mutti and Ricci Lucchi, 1972*).

The sequence stratigraphic analysis was completed by the definition of a prograding-retrograding cyclicity, controlled by the balance between the accommodation space and sediment supply (*Schlager 1993*). This cyclicity is expressed in the variation of the stacking patterns of parasequences (the facies groups of the types defined earlier). Locally these cycles may reflect transgression – regression sequences (TR cycles, *e.g., Johnson and Murphy, 1984; Embry and Johannessen, 1992*). Due to the dominant deep water deposition and the overall absence of coastal onlaps and proximal facies, a direct correlation between the progradation-retrogradation cycles and TR cyclicity was not always possible and therefore the former nomenclature is used for describing all cycles.

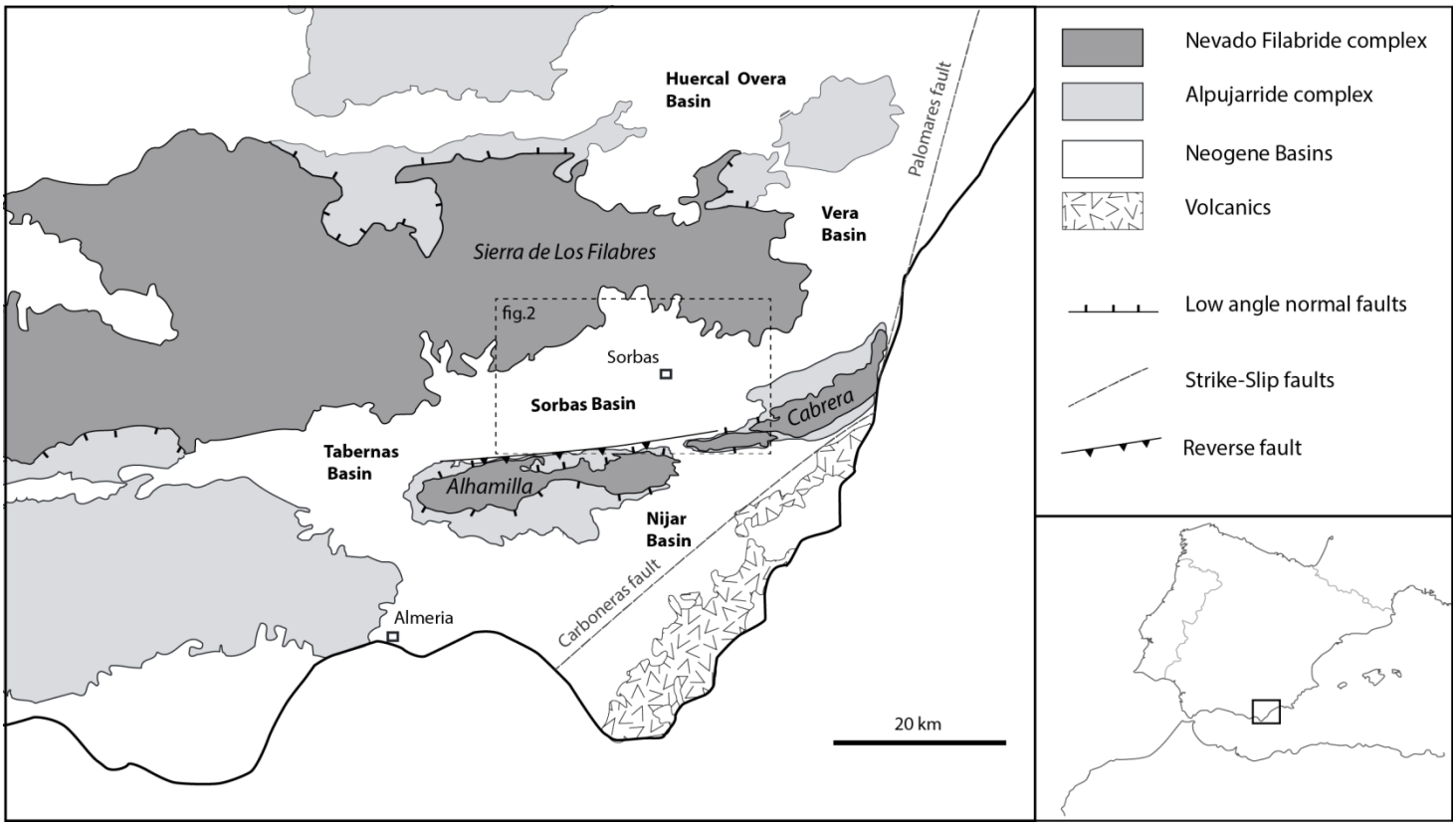


**Figure 1**: Map showing the South-East Betic basins with the major structural features and Sierras with the metamorphic units Of Nevado Filabride and Apujarride. Modified after Augier 2005; do Couto 2014.

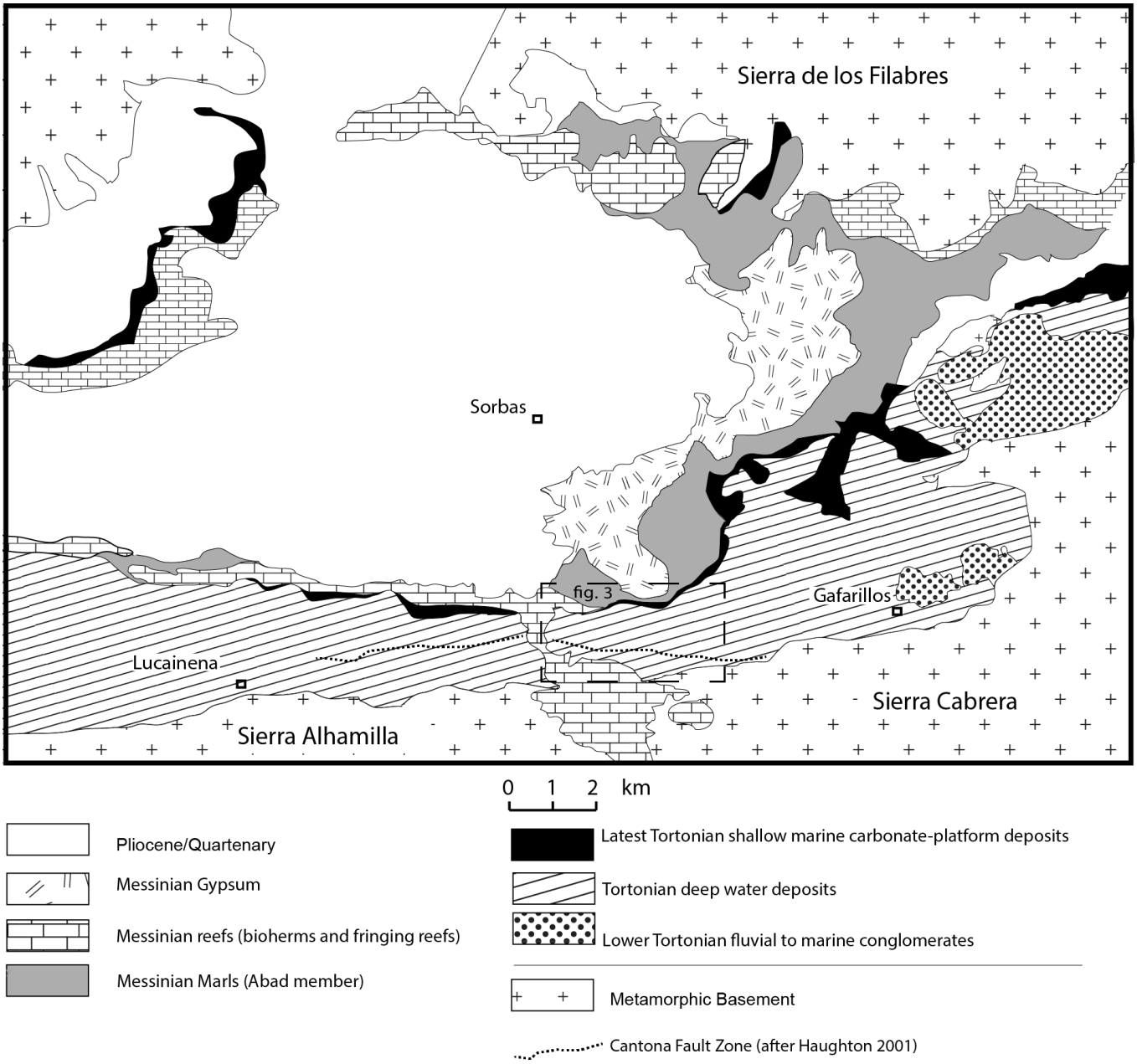


**Figure 2:** Geological map of the Sorbas basin. The study area is marked by the black square. After: Weijermars 1985; Haughton 2001; Puga-Bernabeu 2007.

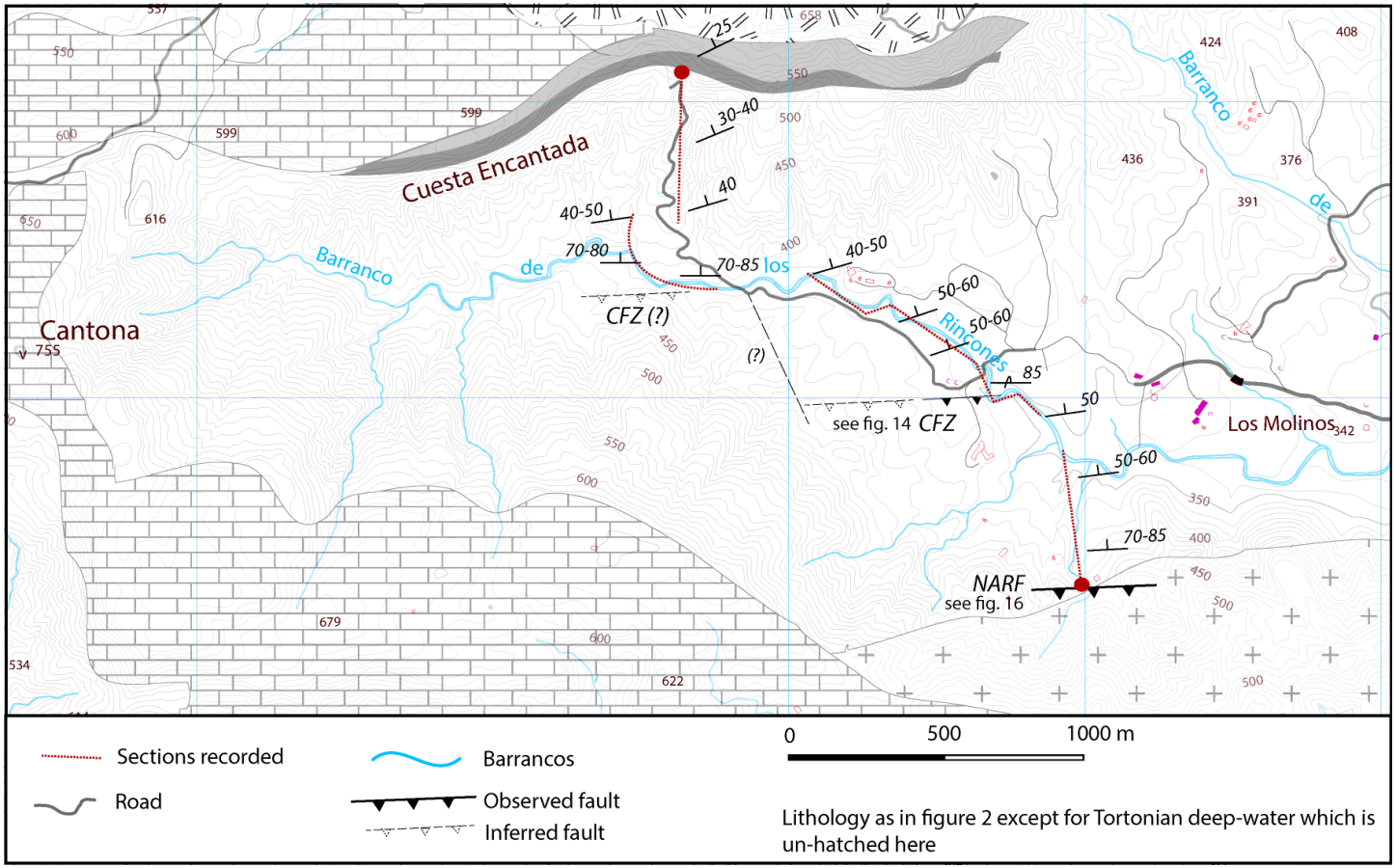


**Figure 3:** High resolution profile from the platform carbonates outcropping on the Cuesta Encantada towards the North Alhamilla Reverse Fault (NARF) in the south with average inclinations of layers recorded. The profile is quite oblique in the middle part while the best exposure was in the Barranco de los Rincones. Near CFZ (?) the presence of the Cantona Fault is expected because of the highly inclined layers but the fault itself was not observed as in the other locality.

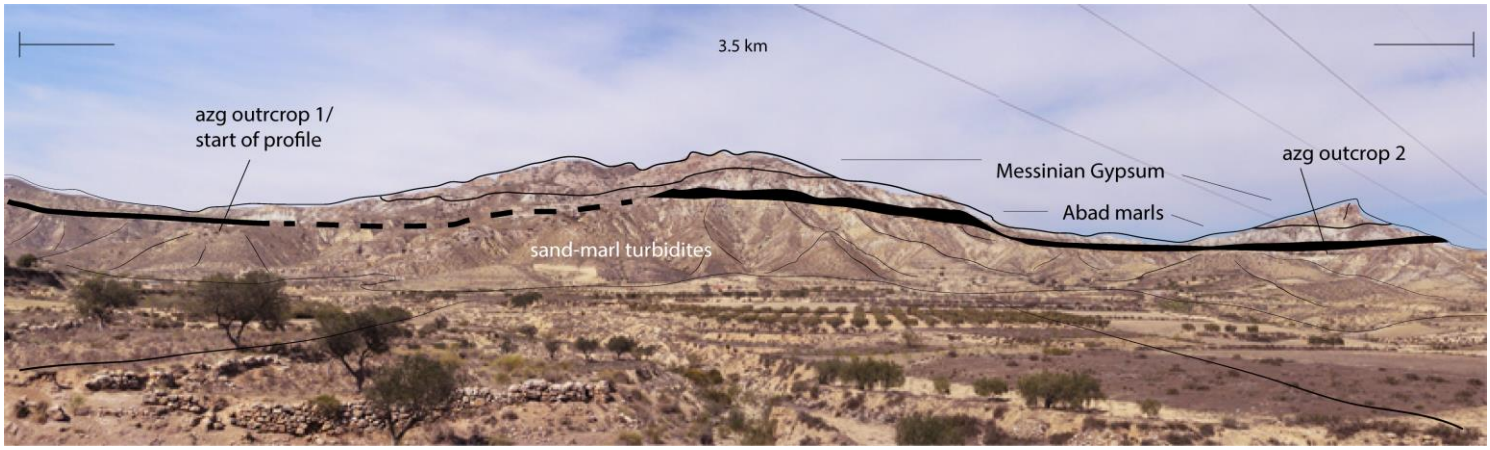


**Figure 4**: Panorama of the E/W trending cuesta (Cuesta Encantada fig.3) where the Latest Tortonian to Messinian sequences of the Sorbas basinfill are outcropping. The bottom half consist of sand-silt/marly turbidites and pelagic marls with directly on top a ridge consisting of platform carbonates (black ridge in the sketch). This unit is followed by the light grey marls of the Earliest Messinian Abad unit and 2 peaks with Messinian gypsum. Also pointed out are the locations of two outcrops where the transition between the turbidites and the platform carbonates has been studied.

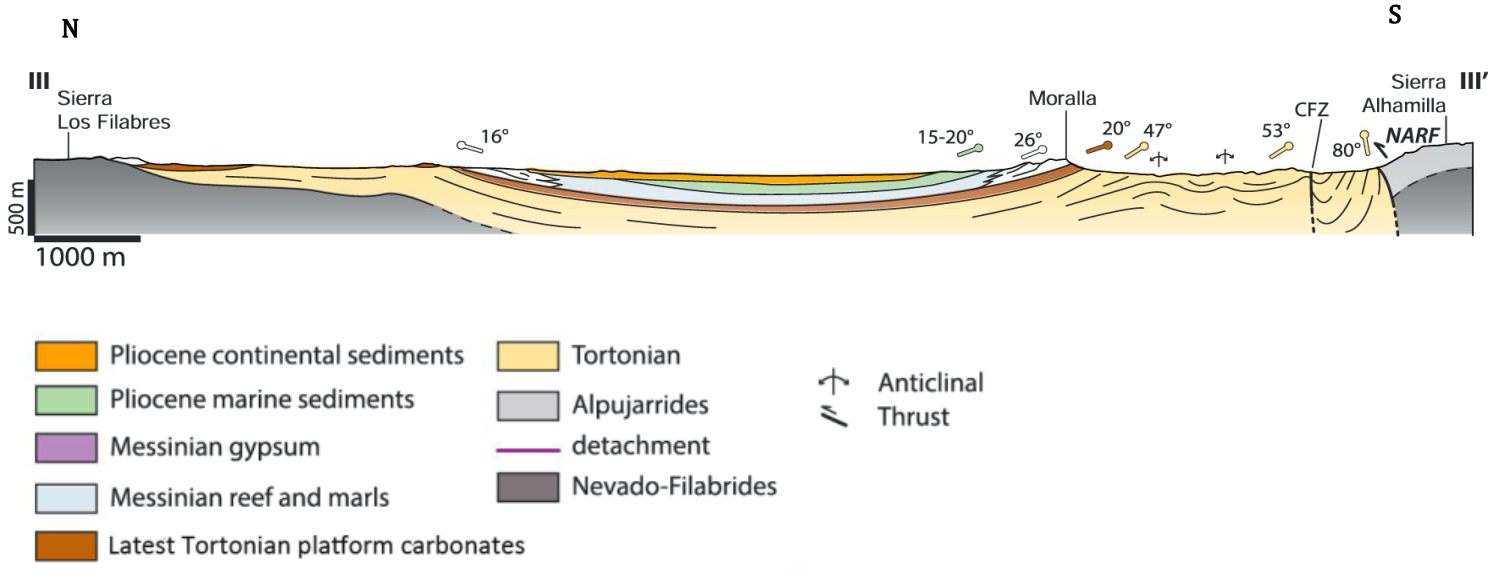


**Figure 5:** synthetic cross-section of the Sorbas basin showing the folding of the basin fill. Modified after do Couto et al. 2014. This section is slightly to the east but very similar to the section in this study. Note the increasingly tilted strata towards the south of the basin where the basement is thrust over the basinfill by the North Alhamilla Reverse fault (NARF). Also note the Cantona Fault Zone (CFZ) which was also recorded in the profile in this research (fig.3, Ch.7).

## 4. Lithofacies groups

Deepwater environments are often complex and built up out of different elements. A high resolution stratigraphy is therefore preferred for a correct interpretation (*Shanmugam 2006*). The section studied in the Sorbas basin proved to be very heterogeneous in turbidite composition, size and internal structures. For recording the stratigraphy throughout the profile a total of 50 different lithological units were defined and described at a cm scale. Each lithological unit was defined on the basis of a fining-upward trend i.e the coarsest point is the base then fining upward until the coarse base of the younger unit above. The types are grouped into lithofacies groups of similar properties. For descriptions and images per individual type see Appendix B.

### Sand-marl turbidites

These types consist of triplets of a basal sand layers, a marl layer and a clay top (fig. 3). The basal sandstone is light brown colored starting with fine or medium sand and fining upwards. Internal structures are either planar lamination or no clear internal structuring (massive sand). The marl layers occur in indurated light grey to white layers and do not contain internal lamination pointing to bioturbation. The base of the units is often flat without significant scouring. Some turbidites contain small bioclastic unrecognizable light colored skeletal fragments especially in the coarse grained units this is more easily visible. Type size is quite variable from 15-60cm, thin bedded to thick bedded. These types only occur in the top 500 meter of the section and do not occur in the lower part. (Types 1, 2, 3, 4, 5, 6, 7, 11, 13, 16, 19)

### Sand-Silt turbidites

Sand-silt turbidites fining up from a basal sand layer to silt and clays are found throughout the entire section. Their internal structures vary however. In the upper part of the section turbidites show massive to planar laminated grading and lacking convolution. In the lower part of the section, the turbidites are generally more complete, grade from massive to planar to convolute and convolution is very pronounced. Some individual units often contain relatively large mudcaps which has been attributed to ponding of the turbidites (Haughton 1994).

*Planar fine sand turbidites:* consists of a 5-10cm mica-rich fine sand base grading into silt and clays. Planar lamination is often present in the silt layer. The base of the type does generally not show scouring but loading structures are observed frequently in type 44. (44 18)

*Planar medium sand turbidites:* Medium sand based types grading normally to very fine sand into silt. Their composition varies but is generally mica-rich. Some turbidites mainly type 9 and 10 can contain small and unrecognizable, light colored skeletal fragments. The base of the layers is often flat and scouring is uncommon. (9, 10, 21, 22, 42)

*Planar coarse sand turbidites:* Normally graded with a coarse sand base of 5-10 cm which is massive to planar laminated. Grading upward into fine sand and-silt and capped by laminated clays. Their

mineralogical composition is variable with very mica rich to very quartz rich mature units. Despite their coarse grain size the base of these units is often quite flat although scouring does occur. (20, 25, 26, 27, 29, 35, 37)

*Convolute fine sand-silt turbidites*: normally graded units consisting of a planar laminated to convolute (very) fine sand layer to silt to a clay layer. These types are ~20cm from base to top and are thinly bedded. The fine sand layer is often only 5cm or less. These units are thin but important in volume mainly in the lower half of the section. (Types 33, 36, 38, 48)

*Convolute medium/coarse turbidites:* sandy generally contains a small 5- 10cm coarse sand layer and then grading to medium-fine sand into silt or clay. The basal sand layer is often enriched in heavier minerals while the finer layers are mica rich. The types contain a massive base which grades into planar lamination and convolute internal structuring. Scouring occurs but infrequently. The silt/clay part is generally 10-20cm large. (Type 24, 34, 43, 46, 47, 49, 50, 51, 54)

### Sandy debrites

These types consist of a relatively large medium or coarse sand part (>20 cm), topped with a layered clay-layer (fig. 6). The types are inversely graded or non-graded and poorly sorted with outsized floating clasts in a matrix. The types often contain a sandy massive (structureless) middle part which is associated with the freezing of the flow. (Types 31, 45, 52, 53)

### Gravely debrites

This group of turbidites consists of a basal gravel layer with grains from a few mm up to multiple cm, a massive coarse to medium sand layer. In the basal gravel layer scouring is common, the sorting is poor and larger clasts are floating in a finer matrix. The very angular gravel clasts are mainly darkly colored dolomites pointing to an Alpujarride source area. The relatively large massive sand deposits are lacking internal structures representing freezing of the flow. If not eroded by a subsequent flow the types are topped by dark grey layered clays. Type thickness is generally >50cm. (t28, 30, 32, 39)

### Megabeds

Megabeds are defined as single types with a sand part >1 meter. There are two main types of megabeds. The first type is light brown to yellow colored, mature quartz-rich in composition and their bases often contain fine gravel size shelf fragments (bivalves/ bryozoans). Often signs of reworking are present within a megabed such as multiple grainsize breaks, and amalgation within an individual bed (fig. 6).

The second type is red-brown colored, mica-rich in composition and very poorly sorted. Often these megabeds contain floating clasts in the matrix or inverse grading which is typical for debrites (*Shanmugam 2006*). The difference between types might indicate a different source for each type.

### Pelagic Marls

Light grey marls which occur in meter scale stacks creating an almost massive marl deposit. The indurated marls are lacking internal lamination indicating bioturbation. The marlstone is occasionally intercalated by small (<5cm) fine sand/silt layers. Fauna found in these marls point to an open marine environment up to several hundreds of meters deep (*Sanchez- Almazo et al. 2001*). (Types 14, 14A)

### Carbonates

The calc-arenite lithofacies was not studied in detail in this study, such detailed descriptions being available elsewhere. The calc-arenite is a prominent feature in the landscape of the Sorbas basin outcropping along an east west trending cuesta (fig. 2 & 4). The calc-arenite unit consists of light colored, well sorted siliciclastics mixed with abundant carbonate platform fossils. The fossil assemblage contains bivalves, bryozoans, oysters, coralline algae and brachiopods. These fossils occur intact in life orientation as well as broken up in storm beds with high concentrations of shell debris (*Puga-Bernabeu 2007*). The thickness of this unit is about 50 meters in the eastern part of the basin while in the section of this study it is approximately 20 meters thick and decreasing further towards the East where it is merging laterally into marls (*Martin an Braga 1990, 1994*).

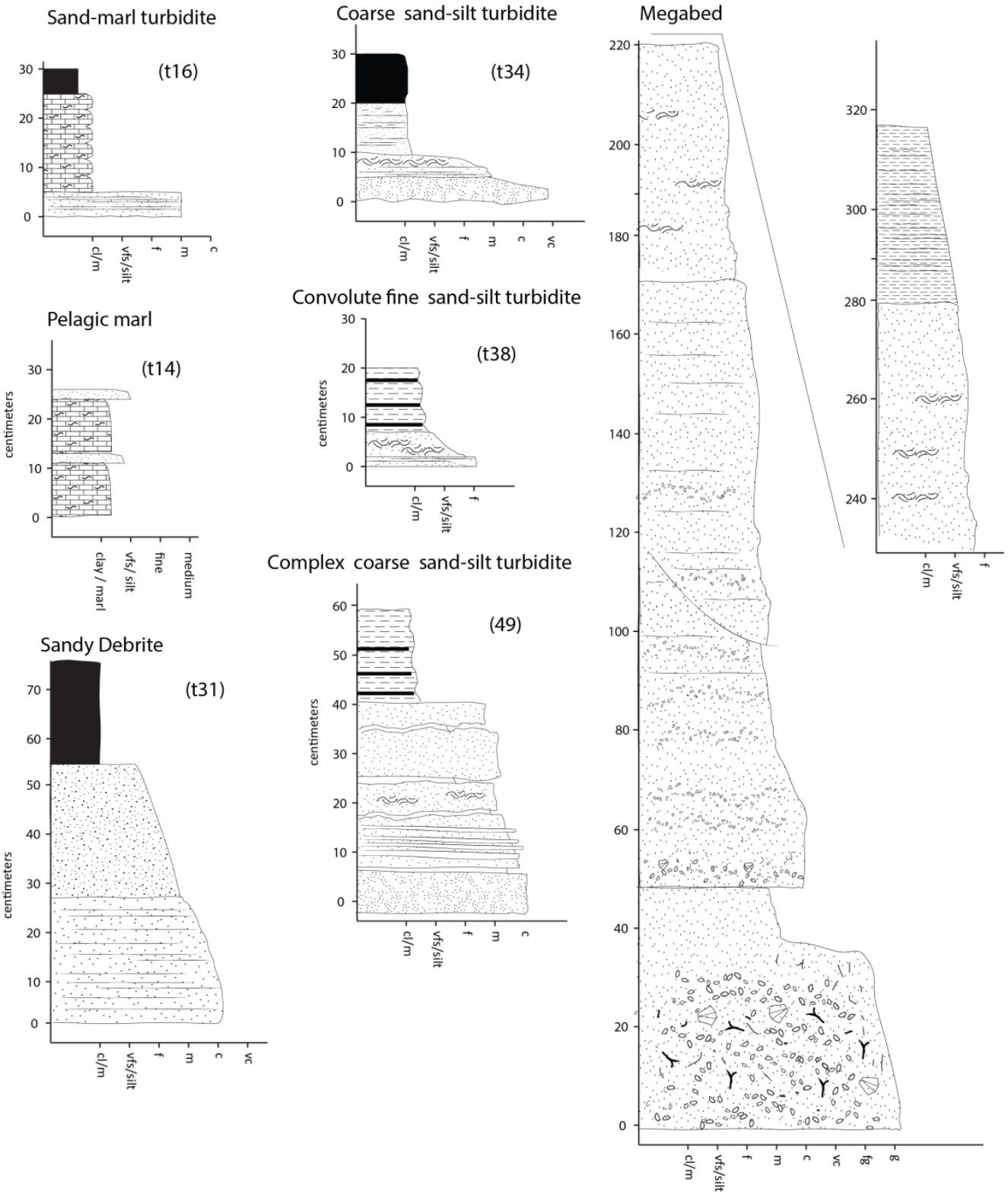


**Figure 6:** Examples from each lithofacies group with grain size depicted on the x-axis. For descriptions of all individual types see Appendix B.

## 5. Facies associations

The lithofacies groups are genetically associated with different depositional systems. The groups are interpreted in relationship with neighbouring units in the high resolution section (Appendix A) and are consequently grouped as facies associations (*Mutti and Ricci Lucchi, 1972*).

### 5.1 Sand-fan

This facies association consists mainly of convolute fine sand turbidites (t48) alternating with convolute coarse-sand turbidites (e.g. t51, 52,) and some sandy debrites (e.g. t53, t45). In addition there is a regular occurrence of megabeds (Appendix A). Gravity-flows are the main process of deposition in this facies association. The turbidites often occur in regular alternations of fine and coarse units. The reworking in the turbidites and megabeds (e.g. t49 and megabed in fig. 6) points to a confined setting where the flows are coming in from the north, are reflected back off the submerged swell of the Sierra Alhamilla and rework the already deposited part of the flow (*sensu Haughton 1994*).

### 5.2 Gravel-fan

Dominated by gravely debrites with some units containing grain sizes up to pebble size these lithofacies groups are associated with a gravel fan (Appendix A, B). Coarse and fine grained turbidites make up the rest of the deposition. Mass transport flows are the dominant process of deposition and scouring is common in-between layers. The clasts in the mass movements are almost exclusively angular dolomites originating from the Alpujarride complex.

### 5.3 Sand-marl fan

Sand-marl turbidites are dominating this sequence with pelagic marls and planar laminated medium sand-silt turbidites making up the remainder. These facies are associated with a submarine fan in which both turbiditic-flows and carbonatic pelagic deposition play a major role. The presence of the marls is a significant difference with the gravel fan and the sand-fan in which this facies does not occur.

The sand-marl fan is laterally continuous. It can easily be followed for several kilometers in the field, outcropping along an east-west trending cuesta (fig. 4). The sequence is often rhythmic in character with respect to the alternation sandstone and marlstone intervals reflecting switching of the mode of deposition between pelagic settling and gravity flows (fig. 7A). Sedimentation rates are probably still relatively high in the sand-rich parts given the loading structures regularly observed. Slumps also occur regularly (fig.7B).

### 5.4 Carbonate platform

The fossil assemblage is associated with temperate climate, shallow water deposition (*James 1997, Braga 2006*). Within the unit different facies are associated with beach/shoal area, inner carbonate factory and a deeper outer factory (*Puga-Bernabeu 2007*). The lack of coral building fossils indicates that temperatures were too low for these reef-builders and no coral reefs were present at the time (*Braga 2006*). The main processes of deposition in this system are in-situ production of carbonates and reworking of (biogenic)

sediments by waves and currents during storms. Sedimentation rates in these carbonate platforms are typically between 70-240 mm/kyr (*Braga 2006 and references therein*). This is in accordance with sedimentation rates in the carbonate platform facies in the Sorbas basin estimated by De Winter and Hartman (unpublished) to be 85-100 mm/kyr. The platform association is grading into marls (lower Abad) upward and laterally to the East (*Martin and Braga 1990, 1994*).

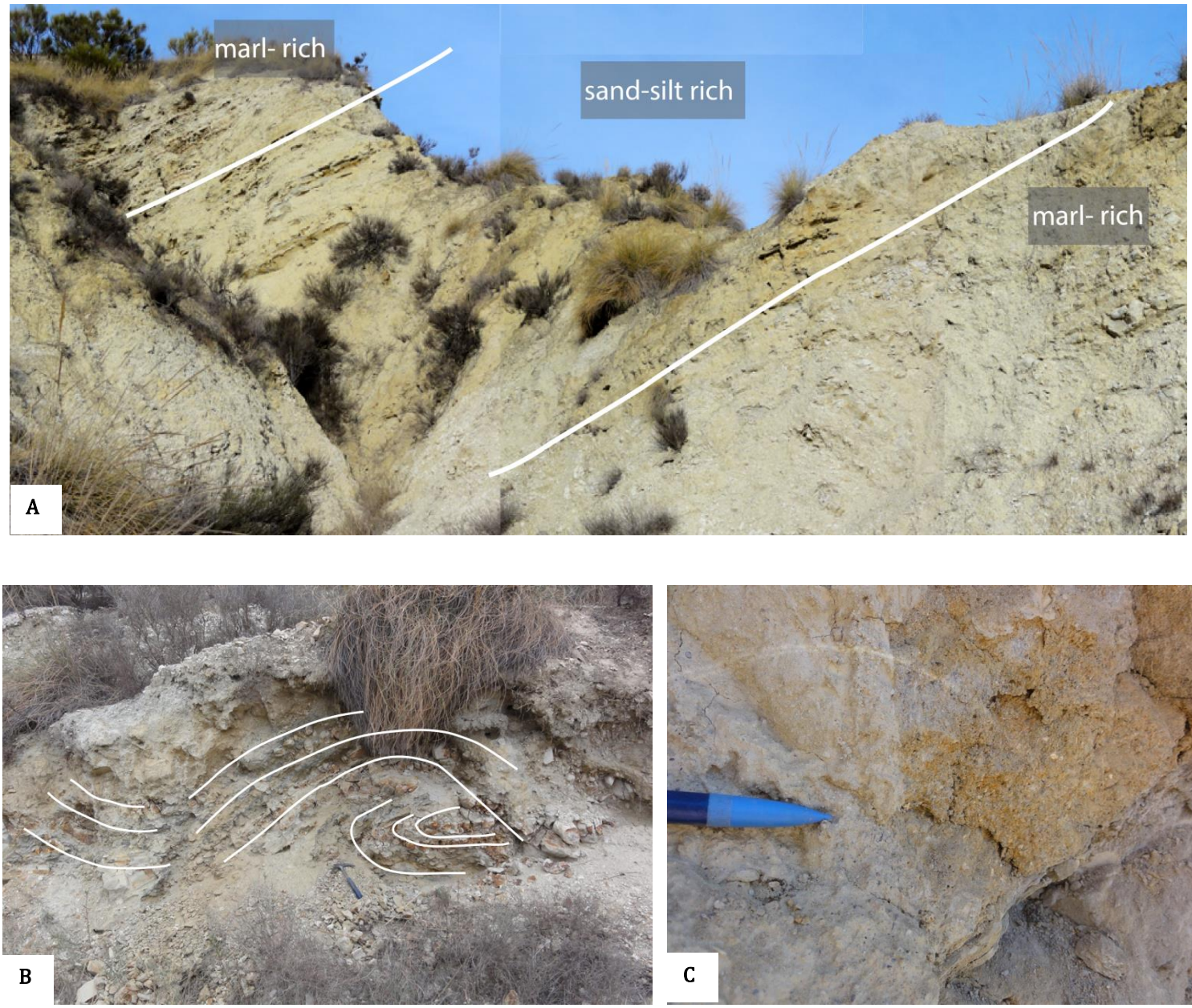


**Fig 7:** field observations **A**: alternations between grey pelagic marls grading into sand-marl turbidites into the brownish sand-silt turbidites. **B**: Slumped level in the marl deposit **C**: sand-turbidite with lightcolored skeletal fragements.

## 6. Facies transitions

The transition between facies associations is gradational. Gravel fan facies associations start out infrequently, become more prominent and then wane again until they disappear (Appendix A). The sand-marl fan associations also enter the sequence in a similar way, from infrequent to being the dominant facies deposited. The transition between the sand fan in the lower part of the stratigraphy, and the gravel fan is unclear as the exposure in the area where this transition supposedly takes place is poor to non-exposed.

*Transition deep-shallow water*

A transition that is apparently sharp is the transition from the deep water to the shallow water platform carbonates. This transition has often been considered an erosional unconformity (*e.g. Weijermars 1985, Martin and Braga 1990*). Field observations however question this interpretation. The transition to the carbonate platform has been studied in several well exposed outcrops. The main observations that lead to think that this is not an erosional unconformity are: (1) the soft sediment deformation structures in the deposits right beneath the carbonatic unit. Flame structures and lenses of carbonatic material are found in the muddy layers below the carbonate unit (fig. 8C). These are indications that the layers below the carbonates were still unconsolidated at the time of deposition of the inner-platform facies. (2) The turbiditic layers below are not cut by the carbonates but are interfingering with the carbonates (fig. 8A, B). From the angle between the turbidites and carbonates the progradation direction was estimated ~NW-W. This interfingering is not always apparent as it is a fast transition and the progradation was to the NW-W while the strike of the outcrop is east west this means one is looking on the strike of the layers. Because some outcrops make a rounded incision the interfingering is partly visible. (3) In the coarser turbidites skeletal fragments are present indicating a bioclastic source area was present during its deposition (fig.7C). These unit might represent the more distal part of the carbonate platform of particles that have been transported downslope.

In addition to these observations, preliminary biostratigraphic data indicates that there is no time missing between the deep water sequences and the shallow water facies (*De Winter and Hartman, unpublished*). This indicates that this limit is indeed a facies limit rather than an erosional or angular-unconformity. The ~10 degree difference in angle is caused by the different angles of the relatively steep turbiditic foresets and the low angle platform topset deposits.

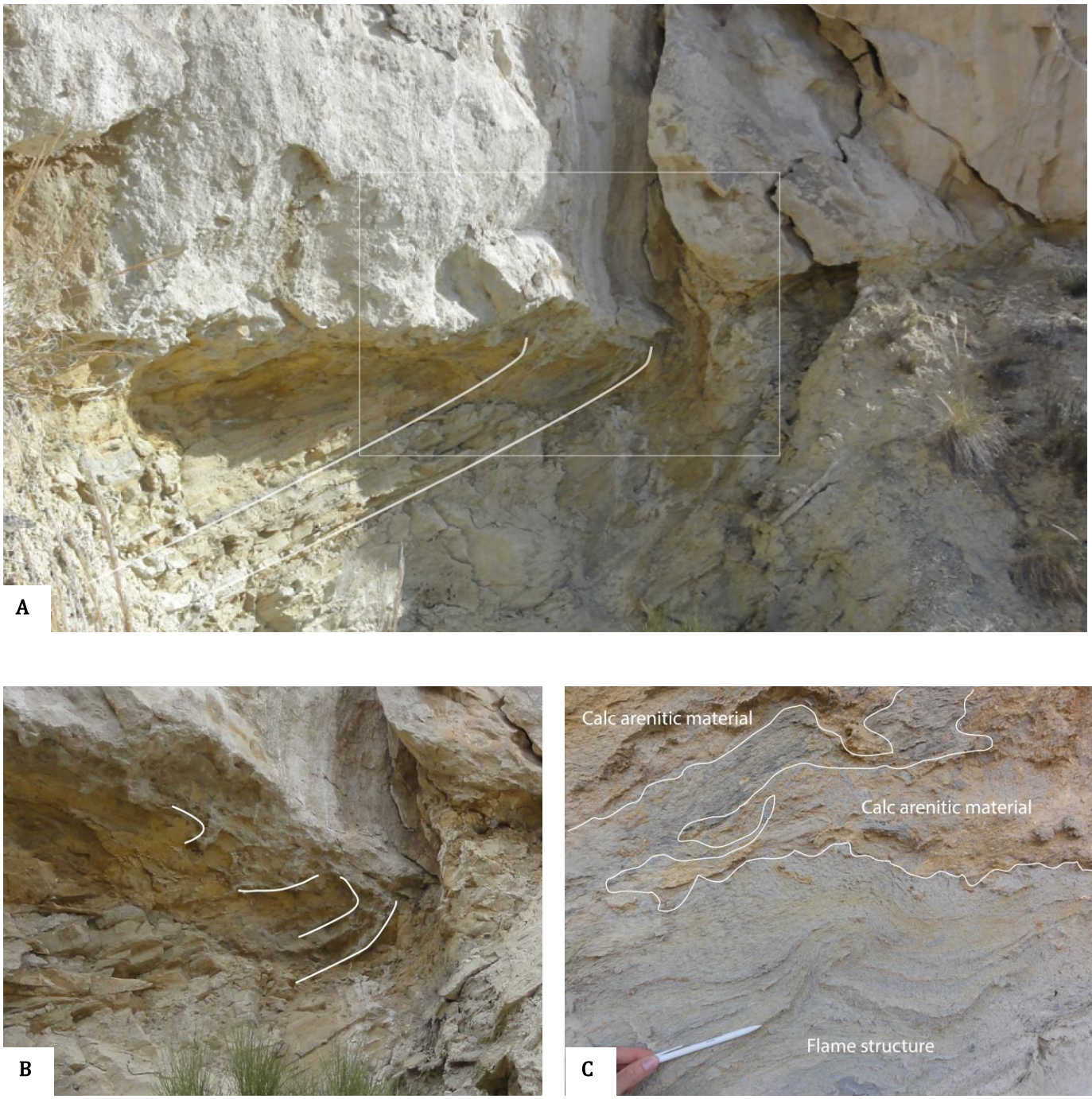


**Fig 8:** Field observations on the transition between the turbidites to the calc-arenite unit. **A:** Tubiditic layers are going into the platform carbonates in an interfingering manner. **B**: zoom in on the contact; note the calc-arenitic material going down in to the muddy layers below under a higher angle of dip. **C**: example of the soft sediment deformation found at Azagador outcrop 2 (fig.4), calc-arenitc material has 'intruded' in the lower mud layer which was still unconsolidated. The flame structure below is another indication of soft sediment deformation.

## 7. Fault analysis

For each fault the sense of movement, direction of movement and the relative timing of faulting was determined. For the determination of the sense of movement, offset and dragging of the layers were used primarily. The direction of movement was determined where possible, by riedel fractures and slickensides. To determine the relative timing of faulting, cross-cutting relationships were used. Because the Tortonian sequence has undergone post-sedimentary tilting, many faults in this sequence are not in their original position anymore. The assumption was made that normal faults originally formed at angles of around 60 degrees in the brittle domain (*Byerlee 1978*).

### 7.1 fault data groups

*Low angle (<40°) dipping faults with a normal offset and kinematics.*

The 1st generation of normal faults is dipping at low angles (<40°) in the field (fig. 9A; fig. 11). The bedding is however dipping between 30 and 70 degrees (fig. 9A, fig. 11, 12). The fault offsets are apparent normal indicating that these cannot be tilted thrusts or reverse faults. After restoration of the bedding to horizontal, these faults are dipping around 60° (fig. 9B and fig. 12) indicating that they were formed previous to the tilting. Offsets in these faults are generally small with most ranging in the order of 10-20 cm although some faults reach up to 1 meter offset (fig. 11, fig. 12). Indications that these faults are syn-sedimentary are: dissipation of the fault offset upwards in the stratigraphy and influence on turbidite geometry. Dissipation of the fault upwards is expected in syn-sedimentary faulting as the created accommodation space is filled by new sediments. After a new phase of faulting the cumulative offset of this younger layer will be less than the pre-kinematic layer. If this cycle repeats, it results in the dissipation of the fault offset upwards in the stratigraphy, as observed in the field. Ultimately, if the fault activity ceases the fault is overlain by a post-kinematic layer. An example of the influence of faulting on the turbidite geometry is displayed in figure 8. The sandy turbidite which is sensitive to relief is emplaced against the tilted block in the depression created by the fault offset. The turbidite has an erosive base and mud lenses are present from the layer below indicating that this lower layer was still unconsolidated (fig. 8).

*Faults with a normal offset dipping at an angle of near 60°*

A 2nd generation younger generation of normal faults is dipping at angles around 60° in the field (fig. 10A, 11). This generation post-dates the first tilting phase in the Sorbas basin. These faults are generally cross-cutting through the whole outcrop and the earlier formed lower angle faults without upward dissipation of the fault offset (fig. 10A, fig. 11).

*Faults with strike slip kinematics dipping 70-90 degrees.*

These faults are dipping steeply in the field and are often associated with drags with subvertical axes and small scale flower structures (fig. 13). No clear evidence was found for syn- kinematic deposition on these strike-slip faults, therefore it is likely that this deformation post-dated deposition in most cases. These steeply dipping strike slip faults post-date the earlier normal faults as often observed by cross-cutting relationships (fig. 11).

*Faults with strike slip kinematics dipping at lower angles*.

In the stratigraphically lower part of the section sinistral E-W trending faults were interpreted to be pre-tilt strike slip fig based on their geometry and kinematics (fig. 10C, fig 15). Before restoring, the drag on the fault is not in accordance with a thrust (fig. 15 zoom-in). After restoring the bedding on these faults, the faults and a drag fold become steep while the slickensides measured remained shallow. These kinematics are in concordance with the fault inclination (fig. 10C). No influence of these faults on the sedimentary deposition was apparent.

*Reverse faults*

Two large dextral reverse faults which are responsible for overturning layers for several tens of meters by dragging locally show a mechanism that has caused the local tilting of the layers in the basin (fig 14). This structure consists of a fold propagation fault with a ramp and flat structure ramp. Directions of movement are quite oblique (fig. 10D). Again the turbidites do not seem to have been influenced during their deposition. The North Alhamilla Reverse Fault (NARF, do Couto 2014) was also captured in our section at the southern border (fig. 16). The basement is emplaced over the Tortonian turbiditic layer which have been dragged to steep inclinations.

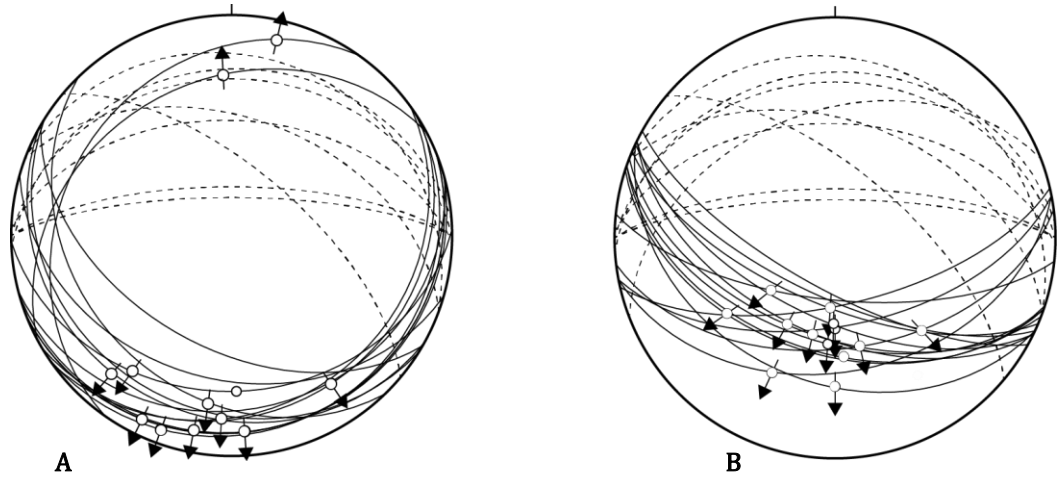


**Figure 9**: Lower hemisphere projections of measured fault planes. The black arrows show direction of motion for faults with normal offset and or kinematics dipping at low (<40°) angles. The dashed lines represent the bedding as measured in the field. **A**: Faults with normal offset as measured in the field note the generally low angle of the planes. **B**: Fault orientations and kinematics after restoring the bedding to horizontal position planes now dipping between 40 and 65 degrees.

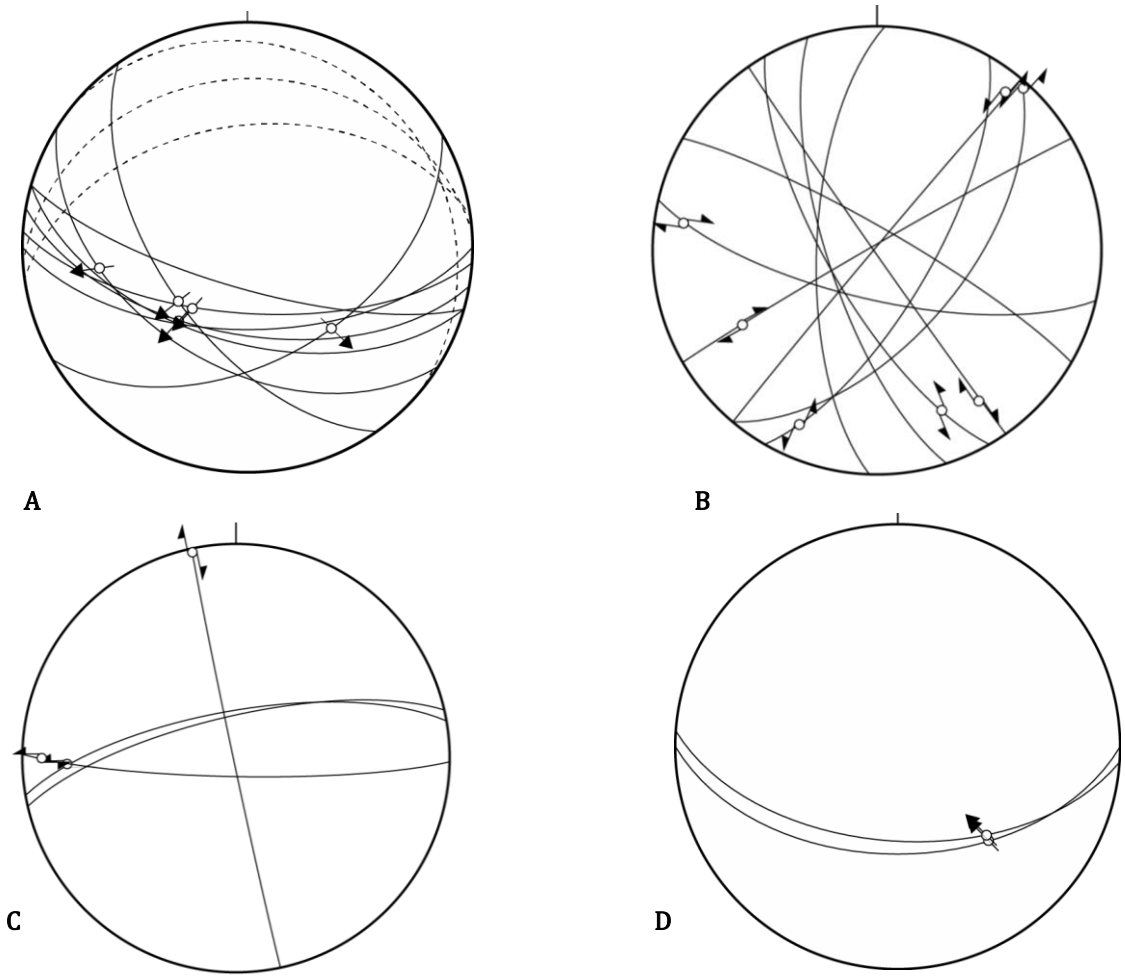


**Figure 10**: Lower hemisphere projections of measured fault planes and directions of motion. **A**: Faults with normal offset found dipping near 60 degrees in the field. **B:** Strike slip faults dipping 80-90 degrees in the field **C:** Stike-slip fault dipping at lower angles in the field in restored position **D:** Dextral, high angle reverse faults (fig.14)

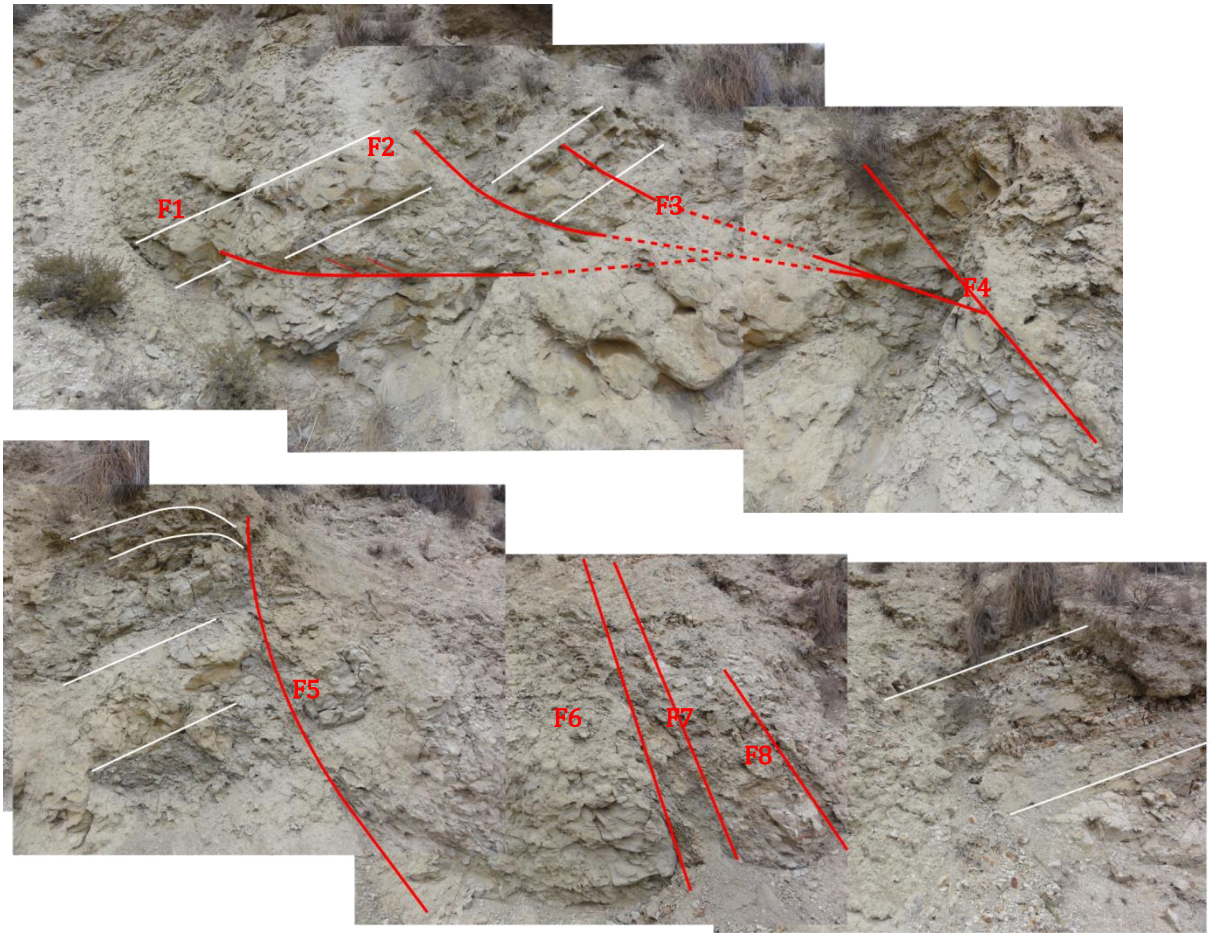


**Figure 11**: Outcrop containing multiple generations of faults. Faults are indicated in red, bedding geometry in white. F123 show normal offsets but are dipping at angles of 12-30 degrees. The offsets are also disappearing as younger layers are unaffected by the fault. After restoring the bedding to horizontal these fault dip at normal angles again. These faults are interpreted as syn-kinematic faults which have been tilted after their formation. F45678 Are normal faults and strike slip faults that are not tilted and therefore formed at a later time. These faults do not show decreasing offset indicating a post kinematic timing of formation.

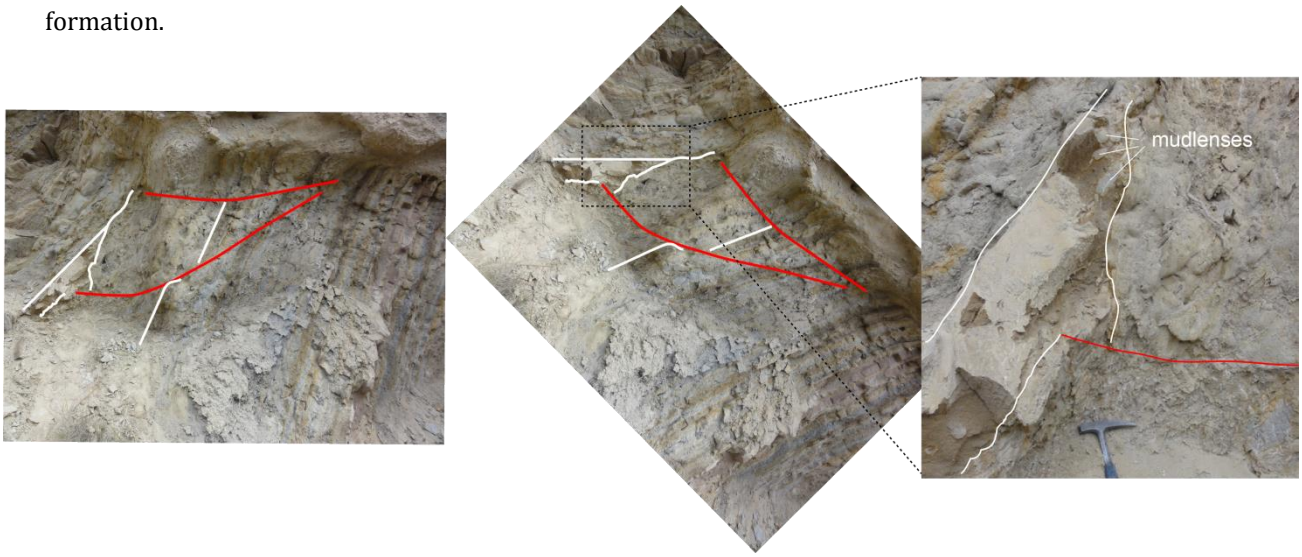


**Figure 12:** Example of a set of syn-kinematic faults which has been rotated by later tilting. Faults are indicated in red, bedding geometry in white. The sandy turbidite which is sensitive to relief is emplaced against the tilted block in the depression created by the fault offset. The turbidite has an erosive base and mudlenses are present from the layer below indicating that this lower layer was still soft. Also note that before restoring the bedding to horizontal the faults are dipping towards the north instead of the south because the bedding had been tilted 70 degrees here. The fault offset and the turbidite geometry dictate however that this must be a syn-sedimentary fault.

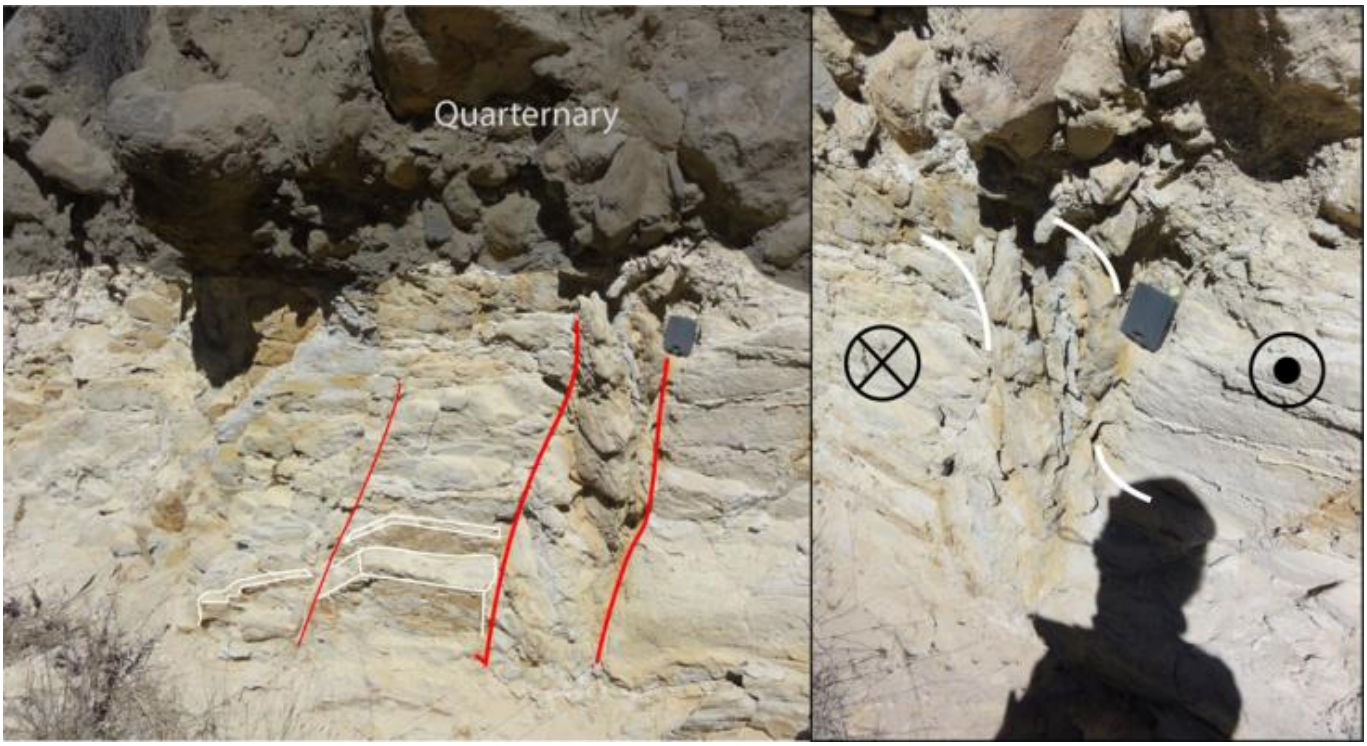


**Figure 13:** Dextral (from drag) steep strike slip fault cutting ~80° dipping layers. The view is perpendicular to the strike towards the north so that one is looking at the bottom of the layers.

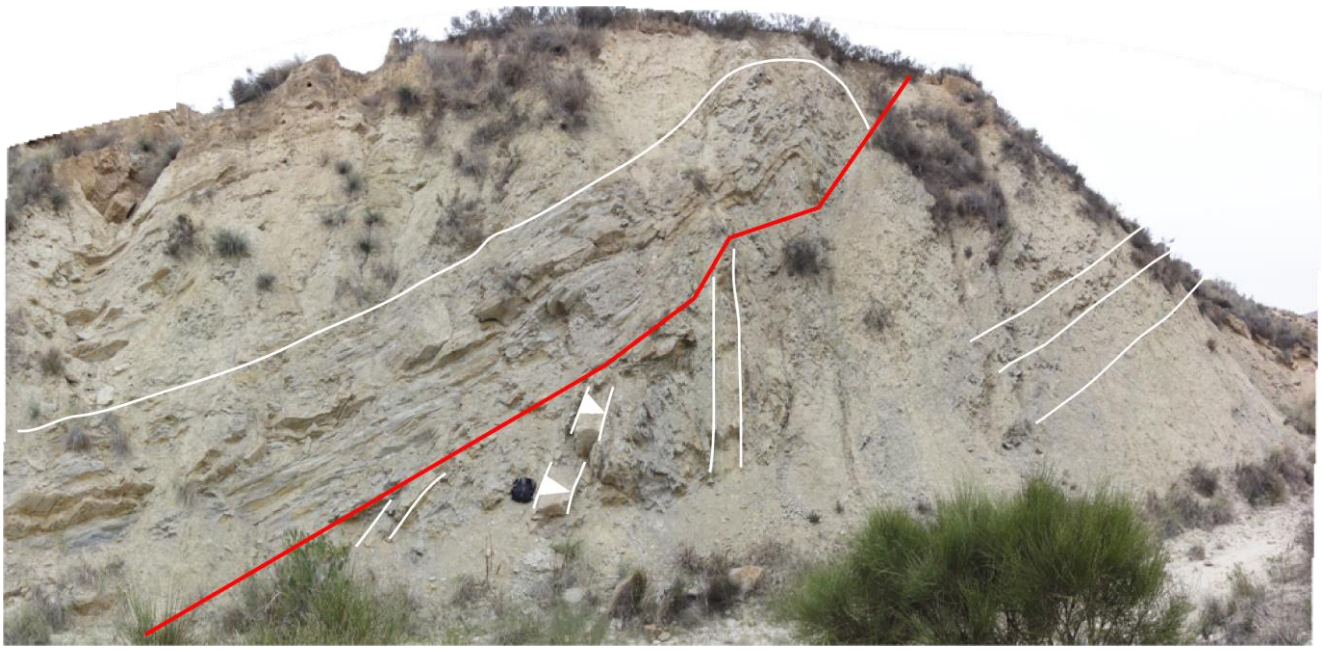

**Figure 14:** Large outcrop looking towards the west onto a dextral high angle reverse fault (fig. 7) with a ramp and flat geometry creating a drag fold which is overturning layers as can be found in the upside down fining sequence (white triangles). The black backpack in the bottom is 40 cm high to indicate scale. The offset is at least 10 meters but likely more.

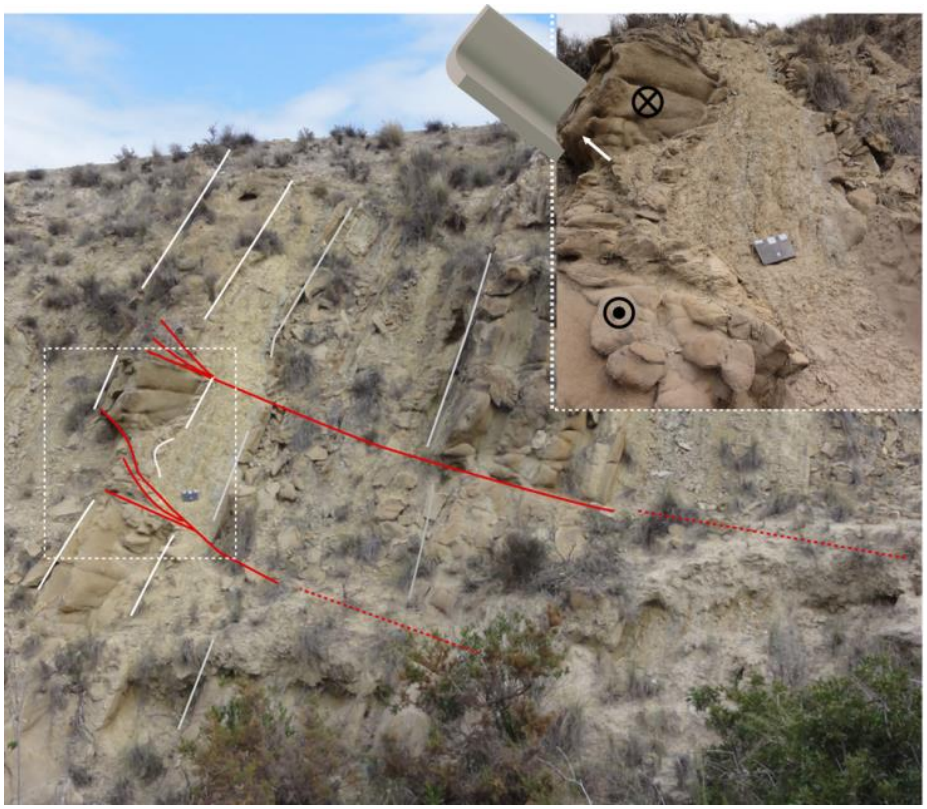

**Figure 15:** Strike-slip fault with small flower structures dipping at a low angle in the field. Vertical (or in this position horizontal) offset is decreasing downward. **Zoom-in:** zoom-in on the flower structure and on a drag with a visualisation of its interpreted 3d geometry. From the drag this fault is sinistral.

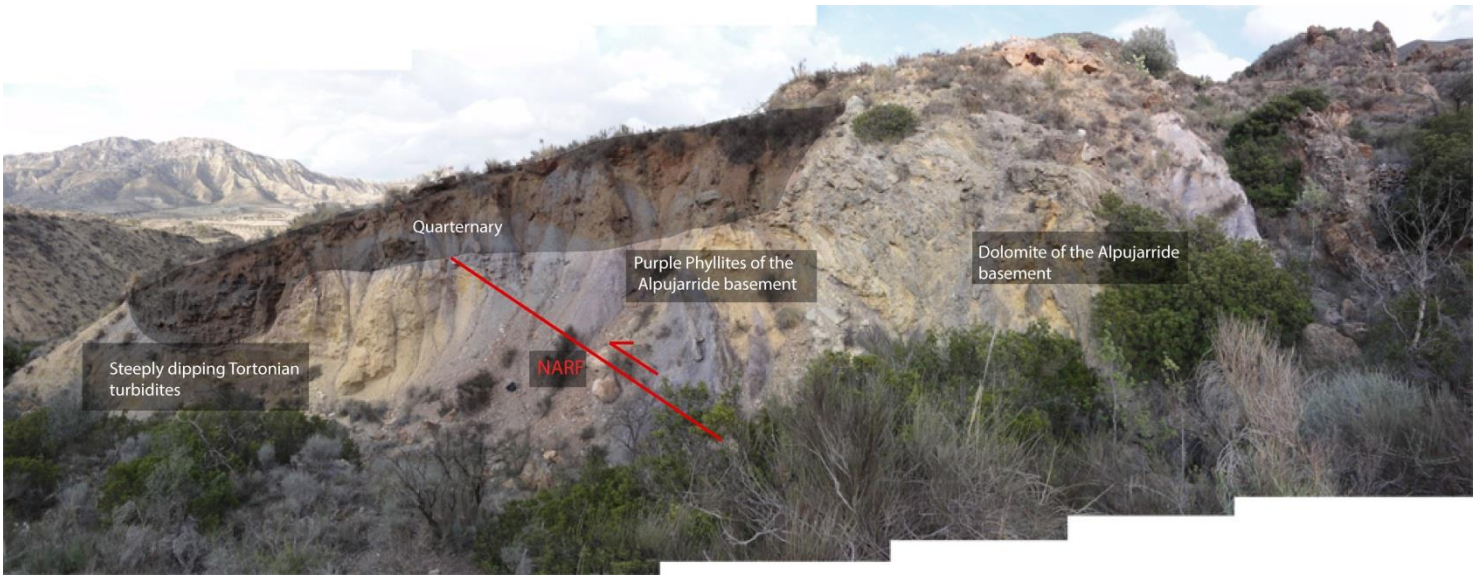


**Figure 16:** North Alhamilla Reverse Fault (NARF) at the southern end of the section (fig. 3). Alpujarride units are emplaced over Tortonian sedimentary units and have dragged these to steep inclinations.

### 7.2 Interpretation of kinematic data

*1st generation of normal faults*

Restoring the original position of the highly tilted normal faults indicates very similar directions of deformation after back tilting suggesting that these faults were formed in response to the same extensional deformation event. The restored geometry of these faults indicates a south-ward dipping direction, suggesting that these faults are antithetic to the main controlling detachment dipping northwards. This type of deformation is typical in the hanging wall to accommodate extension as often observed in asymmetric basins as well as experimental studies (*e.g. Whithjack et al 1995, Song 2001*).

Syn-sedimentary normal faults are found mainly in in the mud-sand fan facies association. The presence of syn-sedimentary normal faults until right underneath and crosscutting the carbonate platform indicates that normal faulting was still active and therefore the basin inversion is unlikely to have caused the transition from a deep to shallow water facies which has been postulated by most authors. In addition to normal faulting, slumps were also encountered in this fan. These slumps are likely to have been triggered by the normal faulting and over-steepening of the muddy slope.

Normal faults are not found in the deposition of the gravel fan facies association and, interestingly, in the lower stratigraphic part of the studied section. This can be a result of decreased deformation during its deposition or to a concentration of offsets along the main boundary normal fault in its vicinity. Several kilometers to the east near Gafarillos (fig. 2), outside the studied high-resolution profile, the density of normal faults increases significantly in the transition from alluvial continental to turbiditic facies found at the base of the basin stratigraphic section (*do Couto 2014*) indicating that normal faulting was also active in the early phases of basin formation. This transition is not exposed along the studied profile.

*2nd generation of normal faults*

No indication could be found that these faults were syn-sedimentary during the Tortonian. When compared with earlier faults, these have not been affected by the tilting of the bedding while the syn-sedimentary faults are. It is therefore likely that these faults formed later and did not have any effect on Tortonian sedimentation.

*Faults with strike slip kinematics dipping at lower angles*.

This is interpreted as a relatively early generation of sinistral strike-slip faults that were affected by subsequent phases of tilting (fig. 15). Cross-cutting relationships with earlier normal faults are absent in the field, but the fact that the strike-slip faults were not associated with syn-depositional patterns in the studied profile infer a post-Tortonian age of deformation.

*Reverse faults*

The oblique directions on the reverse faults (Fig. 10D) indicate that the basin was affected by a transpressional phase causing the oblique movement. Several kilometers towards the east near the village of Lucainena del Torres, E-W trending syn-sedimentary strike slip faults were identified by Haughton et. al (2001). This Cantona fault zone also extends into the Sorbas basin to the location of the

overturned layers in our section (fig. 2). In the Sorbas basin however no evidence could be found for syn-sedimentary strike-slip faulting.

*Faults with strike slip kinematics dipping 70-90 degrees.*

These faults form likely the latest generation of deformation due to the limited influence of tilting on their overall geometry. We interpret these faults as basin splays of the NARF presently situated at the southern basin margin as they are trending at an angle to this main E-W trend. Some Faults are in the proximity of the Cantona Faultzone (which is also E-W trending) are probably linkage faults (fig. 3). The alternative explanation is that this deformation was active much later in the basin evolution and has displaced the CFZ and NARF, e.g. during the Latest Miocene - Early Pliocene (*Stapel 1996*). The former interpretation is more likely as the offset on these faults appears minor and there are no large scale rotations on either side these faults (fig. 3). In both situations, these faults were not active during sedimentation of the studied profile in the Sorbas Basin.

### 7.3 Implications fault analysis

In summary, the syn-depositional normal faults along the studied section indicate that normal faulting was active during deposition in the Tortonian and possibly the earliest Messinian indicated by normal faults cross-cutting the carbonate platform facies base dated at 7.5 Ma. Two main implications are that the subsidence in the basin was controlled by normal faulting and that transition from deep-water to the platform carbonates was likely not forced by tectonic inversion of the basin. This inversion associated with strike-slip deformation and large scale reverse faulting is likely a subsequent deformation phase that took place during the Messinian.

## 8. Sequence stratigraphic framework

The integration of facies, facies associations, paleogeography, basin-geometry and fault kinematic data has allowed the construction of a model of deposition in the Sorbas Basin. Progradation and retrogradation are expressions of the balance between the change in accommodation space (A) over time which is: dA/dt or A' and the change in supply (S) over time which is: dS/dt or S' (Schlager 1993). The model of deposition consists of two settings: One setting in which the creation of accommodation space is larger than the sediment supply (*A'>S'*) and the submarine part of deposition is prograding. The other a setting in which the creation of accommodation space is lower than the change in sediment supply (A'<S') the submarine part is retrograding. We emphasize change in this balance can be either through changes in sediment supply and accommodation as we keep neither constant.

Each setting is associated with a different distribution of the facies groups throughout the basin. A complete environment in this case would consist of a terrestrial part, a shallow marine part and deep marine part. However, no direct field information is available on the terrestrial part of the depositional environments in the footwall as it has been eroded by later uplift. Therefore inferences on the continental part can only be deduced from the composition of the turbidites and the paleogeography.

### 8.1 Shelf / Sand-fan environment

The sand fan is sourced from the north as the Sierra Alhamilla existed merely as a submerged swell. On this northern slope south of Sierra de los Filabres coral reefs on platforms and fan deltas were located (*Braga 2003*). The abundance of fine-grained turbidites (Appendix A) is in accordance with a relatively distal position of a submarine fan and and/or a relatively low slope associated with the hanging wall in asymmetric extensional basins. The asymmetric geometry also dictates that depocenter is located near the hangingwall where the area of largest subsidence is expected to be located (fig. 17).

The abundant reworking and convolution of the beds has been interpreted as the flows rebounding against the submarine swell of the Sierra Alhamilla while being contained in the narrow trough of the basin near the footwall and being redistributed along the basin axis (sensu Haughton 1994). Slope and outer-shelf failure, possibly tectonically induced, occurred regularly releasing the massive amount of sand deposited in the megabeds. These megabeds regularly contain mature sediments and carbonatic skeletal material suggesting that a carbonate platform existed in the proximal part of the basin.

#### *8.1.1 Model of deposition*

In this environment where a shelf exists and the slope is relatively low, the shelf plays a large role in supplying the deep-water (*Blum and Womack 2009 and references therein*). Progradation and retrogradation of the fan is likely correlated to the accommodation space available on the shelf. If this accommodation space is much larger than the supply (A'>S'), by-passing of flow is unlikely and mainly fine grained flows (type 48) are deposited. If accommodation space on the shelf is low or zero (A'<S') and the shelf is emerged with rivers supplying directly to canyons or the slope generating coarse sandy turbidites (e.g. t51, t51, 53), the deep-water fan is supplied leading to progradation of the fan. The model of deposition can therefore be divided into these two end-members (fig. 17).

### 8.2 Alluvial fans / gravel-fan environment

The submarine gravel fan is sourced from the emergent sierra Alhamilla in the south given by the exclusive provenance of very angular dolomite clasts. The coarse grainsize and high angularity indicate a terrestrial part which is dominated by alluvial fan deposition and a high angle slope that transports the coarse grainsize into the deep-water. Such a slope is expected to be formed by the main controlling fault bordering the south of the basin.

The immaturity of the grains also indicates a very narrow hinterland where these fans might reach to the edge of the shelf. If the present day width of the sierra Alhamilla of 5-6km is a good indication of its width during the Tortonian, the shelf must have been only 1-2 km or narrower from the coastline to the steep slope formed by the border fault (fig.18). Shallow-marine facies are not found in this sequence indicating the shelf was never able to prograde for substantial distances.

Since there is also still a source in the north and a basin cross-section of only 15 km is only a small distance for a turbidite to travel (*Shanmugam 2006*) it seems probable that the deposits from the North and south are interfingering as they meet in the depocenter. This is expressed in the heterogeneous composition of the sandy turbidite types pointing to different source areas. The Tortonian turbiditic sequence is not exposed along the northern margin but since the source area in the north has existed for a longer time and is much larger, it is expected that more mature, well sorted, light colored, quartz enriched turbidite types will originate from this margin.

#### *8.2.1 Model of deposition*

If accommodation increases faster than supply (A'>S'), the coarse turbidite and gravely debrite deposition retrogrades and fine-sand-silt turbidites (t38, 36, and 33) are recorded in the profile (fig 18, Appendix A). If A'<S' the gravel facies will start prograding into the basin, debris flows deposit the coarsest units into the basin and erosive channeling is frequent (e.g.t28, t30, 31, 32).

### 8.3 Carbonate platform / Sand-marl fan

Based on the observations on the transition between the sand-marl fan association and the shallow water carbonate-platform (Ch. 6), these two systems were contemporaneous and represent the shallow- and deep-water elements in one and the same depositional environment. Based on the angle between the carbonate-platform and the sand-marl fan (fig. 8), the progradation direction has been estimated towards the Northwest-West which means the source area was likely the Sierra Alhamilla/Cabrera. The shallow marine carbonate platform facies is unique in the basinfill as these do not occur below this one unit. We interpret this as the final stage of the filling of the basin and progradation into the basin did not occur until the basin had become shallow enough. The transition from the alluvial fan/gravel-fan environment to this environment is therefore envisaged to have happened in two stages:

*8.3.1 Phase 1*

In the hangingwall deep-water facies associated with the gravel-fan disappear while facies associated with sand-marl fan appear marking the transition between these two systems (Appendix A). Meanwhile, the shallow temperate carbonate-siliciclastic platforms were possibly already located only on the partly submerged footwall of the sierra Alhamilla/Cabrera. Since the Sierra Alhamilla is presently only 5-6km wide, these platforms must have been only 1-2 km or narrower from the coastline to the steep slope formed by the border fault in the early phase of this environment (fig. 19). This steep slope prohibits the platform facies from prograding into the basin. The sedimentation rate in the carbonate-platform is too low (Ch. 5.4) to fill the accommodation space available. The turbidites keep bypassing the platform and steep slope during high sediment supply and are deposited in an aggrading fashion in the basin. Such a disconnection between a footwall platform and the basinal facies in the hangingwall has also been proposed by Fabbi and Santantonia (2012) for early Jurassic half-graben in the Northern Apennines.

Any evidence that these platforms existed on top of the sierra has been eroded by later uplift. On the South side of the sierra Alhamilla the carbonate-platform facies is found on top of metamorphic basement bordering the basin (*Nijar basin, see Fortuijn and Krijgsman 2003*) indicating that there might have been a similar setting on the northern flank of the Sierra aswell.

*8.3.2 Phase 2*

During the second phase the basin has become shallow enough for the carbonate-siliciclastic platform to start prograding into the basin (fig. 19). Deposition occurs in large scale clinoforms with platform carbonate topsets at low inclinations and steeply inclined turbiditic foresets. While the clinoform slope is still quite steep the break in slope is still restricting the progradation of the platform facies. A similar model of a distally steepening ramp has been proposed by Braga (2006) but has not been applied to the Sorbas Basin. For the deep-water deposits the slope is now however less steep than the slope that was formed by the main controlling fault. A lower slope is generally associated with finer grain sizes (e.g. Reading & Richards 1994) while there is less potential energy for the gravity flows (fig 19). In this sense, by this decrease in slope the filling of the basin itself could explain the gradual transition from the gravel-fan (high energetic) association to the sand-marl fan (low energetic) which lacks gravel types.

*8.3.3 Model of deposition for the deep-water part*

When (A'>S'), the sandy turbidite facies are retrograding. The basin becomes starved of siliciclastic input which allows the carbonate factory to thrive and the pelagic marls are deposited as drapes in the whole basin. If (A'<S') the basin is again supplied with siliciclastics and the sand-marl and sand-silt turbidites facies are prograding into the basin (e.g. t2, t3, t16, 13, t10).

Retrogradation

A'>S'

Submerged shelf

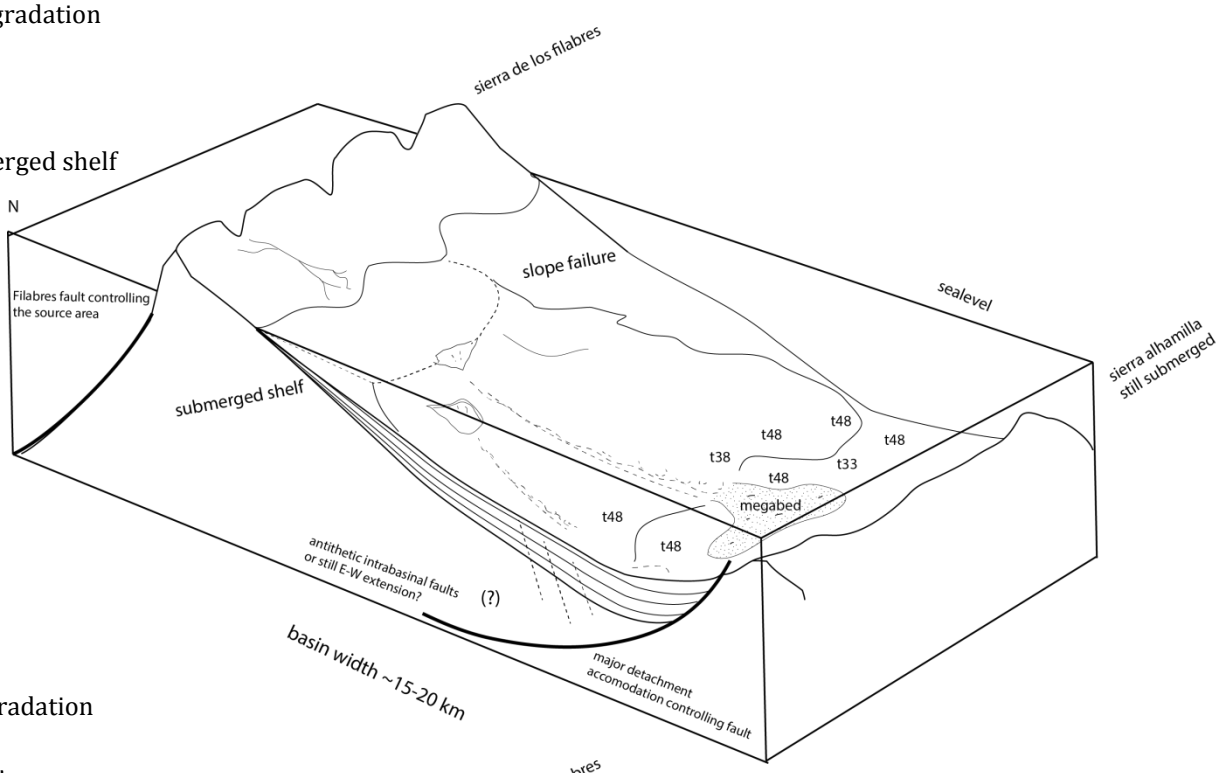


Progradation

A'<S'

Emerged shelf

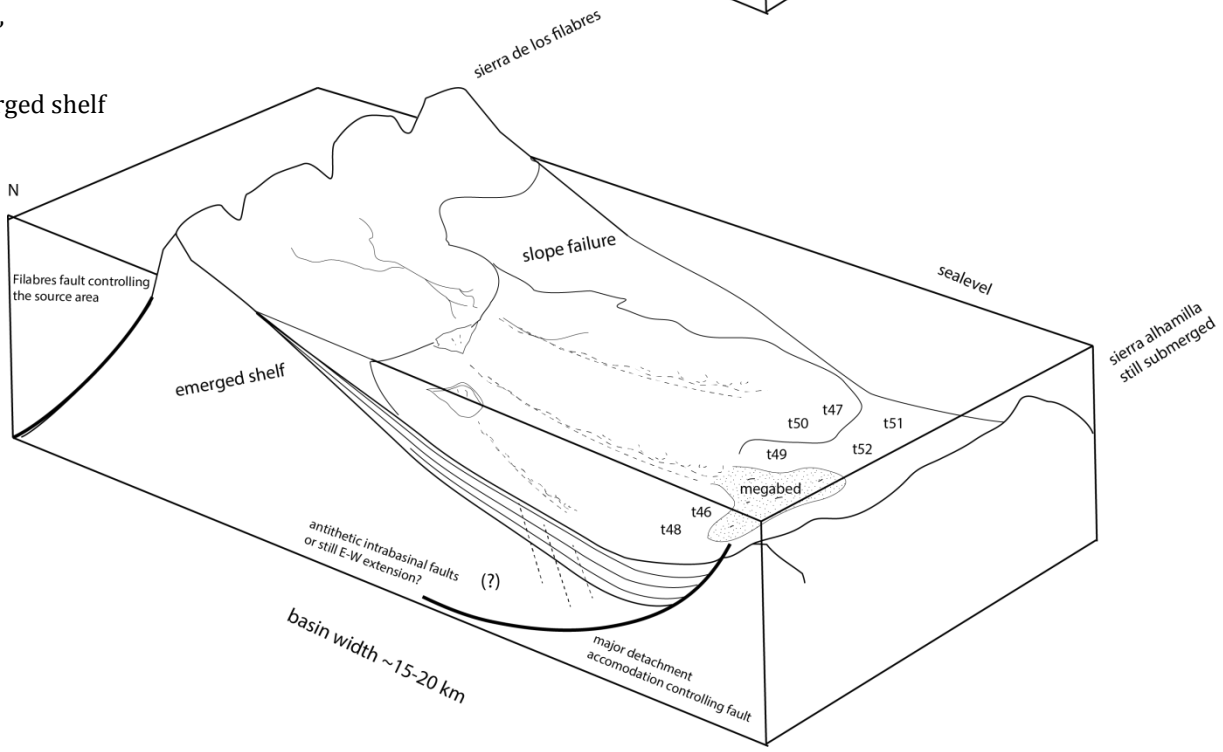


**Figure 17**: Depositional model for the sand fan environment. During retrogradation coarse material does not bypass the shelf with the exception of mass transport by slope failure. Fine-grained turbidites sourced from the north reach the southern border showing abundant convolution structures. During progradation the coarse turbidites bypass the shelf and are deposited in the depocenter where they are ponded showing signs of reworking. The types associated with progradation (A'<S') and retrogradation (A'>S') are put into the environment (t46, t52 etc.).

Progradation

A'<S'

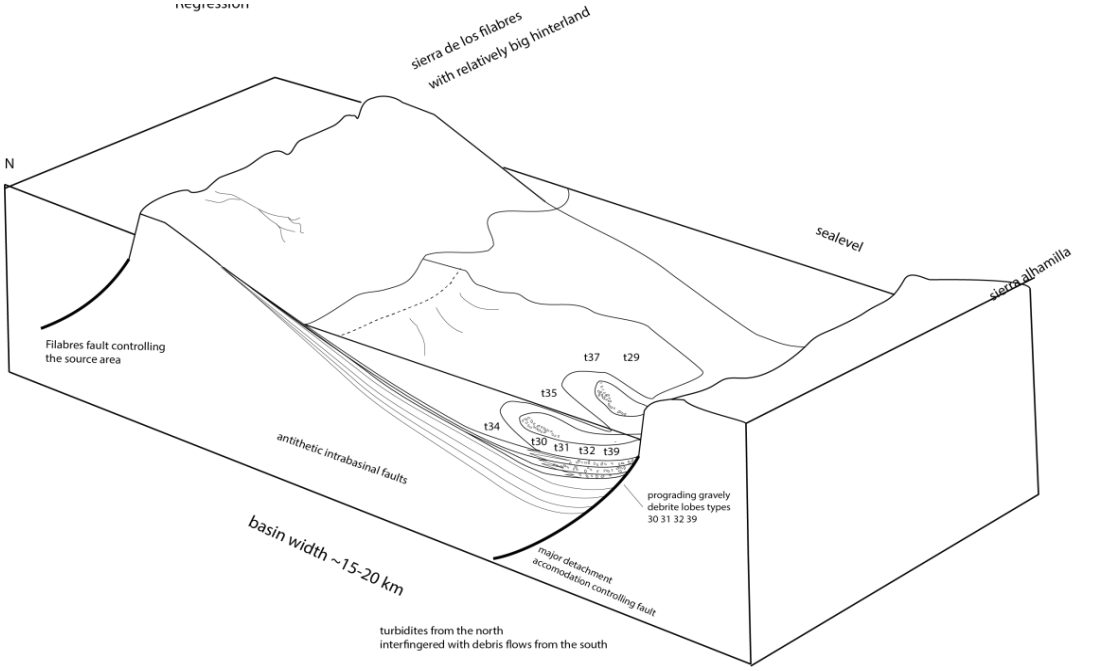


Retrogradation

A'<S'

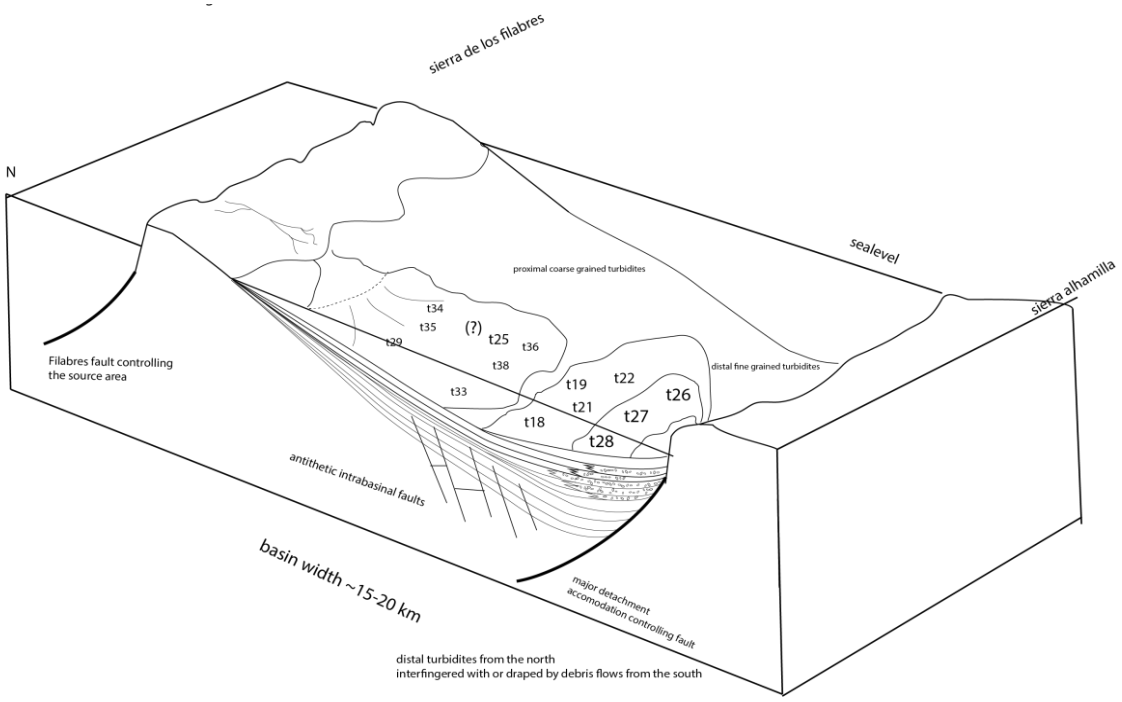


**Figure 18:** Alluvial fans to gavel-fan environment. The Sierra Alhamilla is now emergent and providing coarse angular clastic to a gravel fan which is prograding towards the north. It is interfingering by coarse turbidites sourced from the North which might occasionally reach the other side of the basin. During retrogradation the gravel deposition is pushed back landward and only sporadic flows reach further in the basin. Gravity flows are dominant again and coarse sand-silt turbidites are deposited proximally while fine sand-silt turbidites are deposited distally.

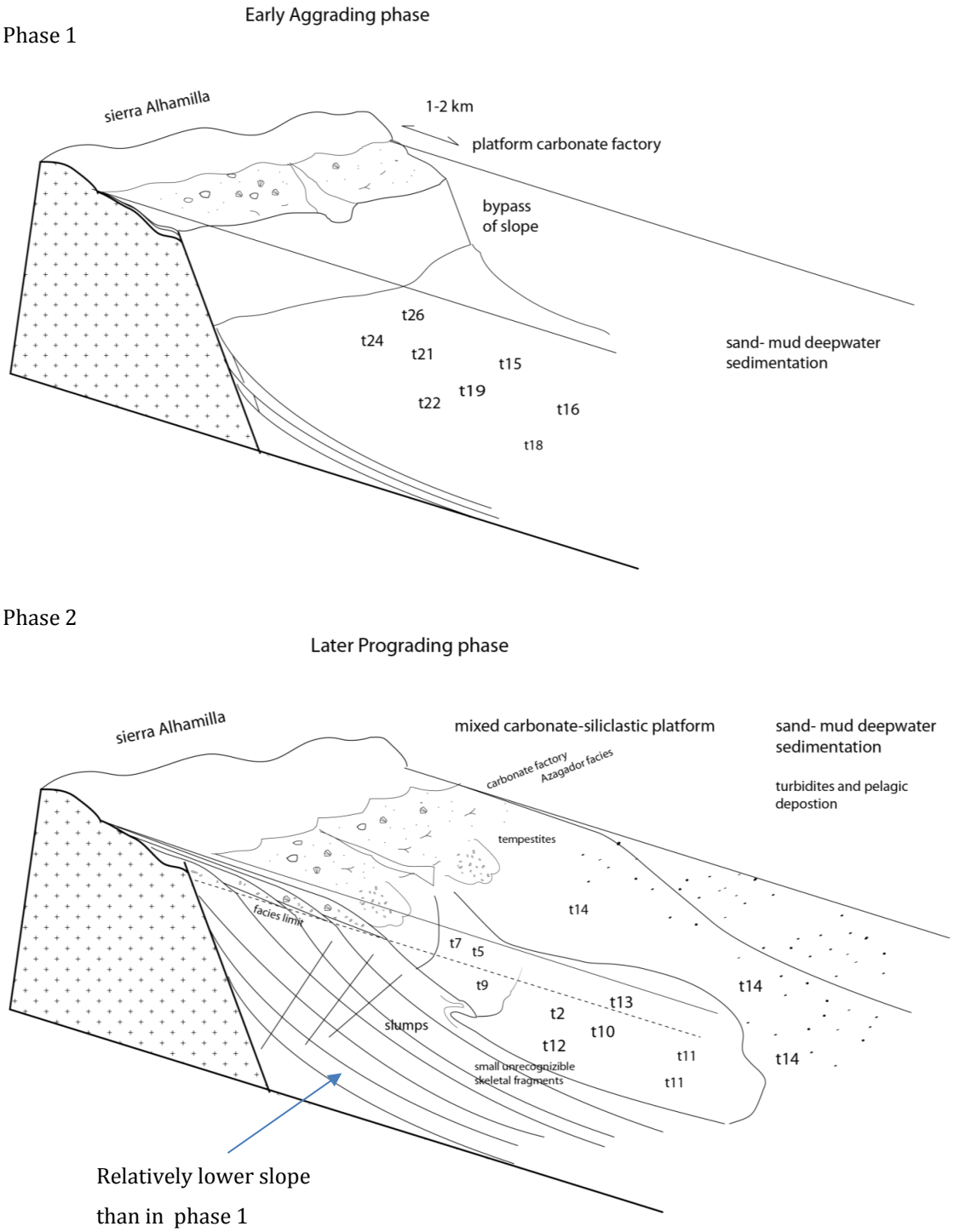


**Figure 19:** Depositional model for the final phase of the Tortonian basin fill. Note that these images are drawn in a different orientation as the previous models as it is now facing Sierra Alhamilla in the south.

Phase (1) A shallow water platform has developed on the sierra Alhamilla but the steep slope and deep basin prevent it from prograding. Meanwhile bypassing flows are aggrading at the base of the slope.

During phase (2) the basin has been filled up more and the water depth is shallow enough for the platform to prograde while on the slope and distal part the turbiditic and pelagic sedimentation continues. Note that the slope of the clinoforms is still steep but less steep than in phase 1 meaning less potential energy in the gravity flows which could explain the fining upward sequence. Partly after Braga 2006.

# 9. Cycles

The relative changes in accommodation and supply are expressed in the variation of parasequence stacking patterns which form progradation and retrogradation sets. Combining the model of deposition with the high resolution column (Appendix A) progradation and retrogradation sets can be defined and subsequently cycles can be defined. Progradation-retrogradation cycles at different scales could be defined. Cycles of different scales can be distinguished on the basis of their relative importance in facies change. The Sorbas basin fill can be consequently divided into at least two *Major* progradation-retrogradation cycles of 400-500 meters constituting the changes in environment. These cycles can be divided into *Intermediate* cycles of 20-150 meter. Lastly, *Minor* cycles are defined of meter scale.

## 9.1 Cycles in the Shelf to Sand-fan

### *9.1.1 Parasequence stacking patterns*

Progradation set: starts with fine grained convolute sand-silt turbidites followed by coarse sand-silt turbidites and finally sandy debrites and megabeds (fig. 20; Appendix A). In the retrogradation set the parasequences are stacked inversely starting from the sandy debrites and megabeds to coarse turbidites and finally convolute fine grained sand-silt turbidites.

### *9.1.2 Major cycle 1*

A major cycle was not definable as there is no clear trend in the stacking patterns at larger scale. Also it is not really clear where the facies transition occurs from this environment to the other.

### *9.1.3 Intermediate cycles*

Several intermediate cycles could be defined (Appendix A). These progradation-retrogradation cycles have a stratigraphic thickness of ~20-40m. These cycles are marked by a strong asymmetry (fig. 20). The progradational set within each intermediate cycle is relatively thick in terms of stratigraphic thickness while the retrogradational set is relatively thin. The megabeds can either be interpreted as the top of a progradational set while in other cases the stacking pattern above and below these bed do not show a progradational trend preceding the bed nor is it followed by a retrogradational one (fig. 20). The latter would indicate that they were created by a single event such as slope failure (Appendix A).

Triggering of mass movements by seismicity or steepening of the slope is a process which might be expressed in the Sorbas basin in the regular occurrence of these megabeds. Such occurrence of seismically induced deep-water deposits has been inferred by multiple studies (e.g Gorsline 2000, Goldfinger 2003). The Gordo Megabed in the neighboring Tabernas basin is also possibly linked to seismic activity (Kleverlaan 1987).

### 9.2 Cycles in the alluvial fan to submarine gravel fan

*9.2.1 Parasequence stacking patterns*

The stacking pattern of a progradational set starts with deposition of fine grained sand-silt turbidites (Appendix A) these are followed by coarse turbidites (e.g. t34, t26, t27) and finally deposition is dominated by gravely debrites (e.g.t28, t30, 31, 32). Sedimentation is increasingly dominated by the deposition of gravely debrites and coarse turbidites. A retrogradational set is the inverse pattern of the progradation creating a stacking pattern of gravely debrites to coarse turbidites to fine grained turbidites upward in the stratigraphy.

*9.2.2 Major cycle 2*

Major cycle 2 is marked by large scale progradation set of increasing deposition by gravely debrites, followed by a retrogradation stacking pattern marked by a general decrease in gravely debrite deposition and ultimately a transition to the sand-marl facies which is lacking gravely debrites (fig. 21).

*9.2.3 Intermediate cycles*

Two intermediate progradation cycles could be distinguished within major cycle 2. The stratigraphic thickness of these progradation-retrogradation cycles is ~100-150 meter and is marked by a strong asymmetry. The progradational set within each intermediate cycle is relatively large in terms of stratigraphic thickness while the retrogradational set is relatively short. In the first intermediate cycle some smaller cycles could also be defined of 15-30 m (Appendix A). In the second intermediate cycle this distinction is harder.

### 9.3 Cycles in the Carbonate platform to sand-marl fan

*9.3.1 Parasequence stacking patterns*

A progradational set starts with marl-types (14) and then towards sand-marl turbidites (1, 11, 13, 16) to sand-silt turbidites (2, 10, 9) (see Fig. 20 and Appendix A). It is thus marked by a relative increase in siliciclastic deposition by turbiditic flows. Retrogradational set: the frequency of sand-silt turbidites decreases and mixed sand-marl turbidites are more frequent, finally pelagic marls (14) are deposited again (fig. 20, Appendix A). The retrogradational set is increasingly dominated by pelagic sedimentation.

*9.3.2 Major cycle 3*

Major cycle 3 is a large scale progradation from the deep-water sand-marl facies associations towards the shallow-water marine platform carbonates which is followed by a retrogradation to deep-water marls (fig. 21).

*9.3.3 Intermediate cycles*

The stratigraphic thickness of the intermediate cycles is ~20-30m for each progradation-retrogradation cycle (Appendix A). The cycles are of a sinuous shape of gradual transgression and regression as the units change from pure sand to a mixture of sand and pelagic marl to pure pelagic marl deposition. The cycles cannot be correlated directly to individual faults in the basin as the influence of these single faults is small (see Minor cycles below).

A problem with the turbidite sequence is the poor time constraint available which makes it hard to calculate cycles. For the intermediate cycles within major cycle 3 preliminary biostratigraphic data is available. The upper part of the major cycle 3 has been dated by de Winter and Hartman (unpublished) who found a dextral sinistral coiling change of *G. scitula* dated at 7.584 Ma (*Hüsing 2008*) in turbidites 135 m below the calc-arenite unit. By astrological tuning they dated the turbidites just below the calc-arenite 7.524-7.476Ma. From this timing the average sedimentation rate is calculated to be 1.25-2.25 m/kyr. This is an indication for the sedimentation rate in the sand-marl fan environment. However given the difference in sedimentation processes in the in the other depositional systems, sedimentation rates are probably different.

Dividing the thickness of the cycles by the sedimentation rates, the duration of a cycle in this environment lies in the domain of cyclicity controlled by precession (19-23kyr)

*9.3.4 Minor cycles*

Minor cycles of meter scale could be defined and can be correlated directly to the activation of individual intrabasinal faults (Appendix A). On outcrop scale the normal faults can be seen to cause a quick transition to types associated with retrogradation that are deposited above the fault (Appendix A). This indicates that faulting is influencing on the deposition of sediments. The space created by the normal fault can however be filled by a single turbidite flow such as seen in an example of syn-sedimentary faulting found (fig. 12). If it is considered that the faulting activity in these antithetic small scale faults indicates movement of the larger controlling boundary fault it explains the short term fining in the subsequent layers above the turbidite that immediately fills the fault. The fining is however in many cases not long lasting (Appendix A) which is probably due to a relatively high rate of deposition to the subsidence.

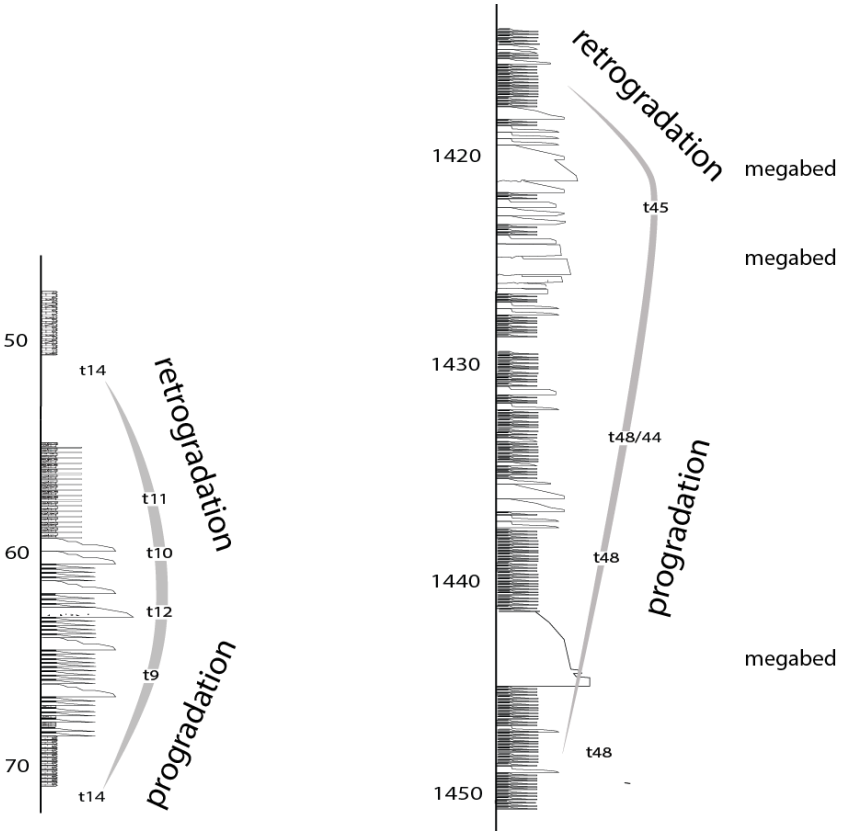


**Fig.20**: Examples from Appendix A showing stacking patterns of the types resulting in progradation and retrogradation sets. A: the stacking pattern from pelagic marls (t14) associated with A'>S' to sand-silt marls associated A'<S' results in progradational set. Note the lowest megabed in the right column is

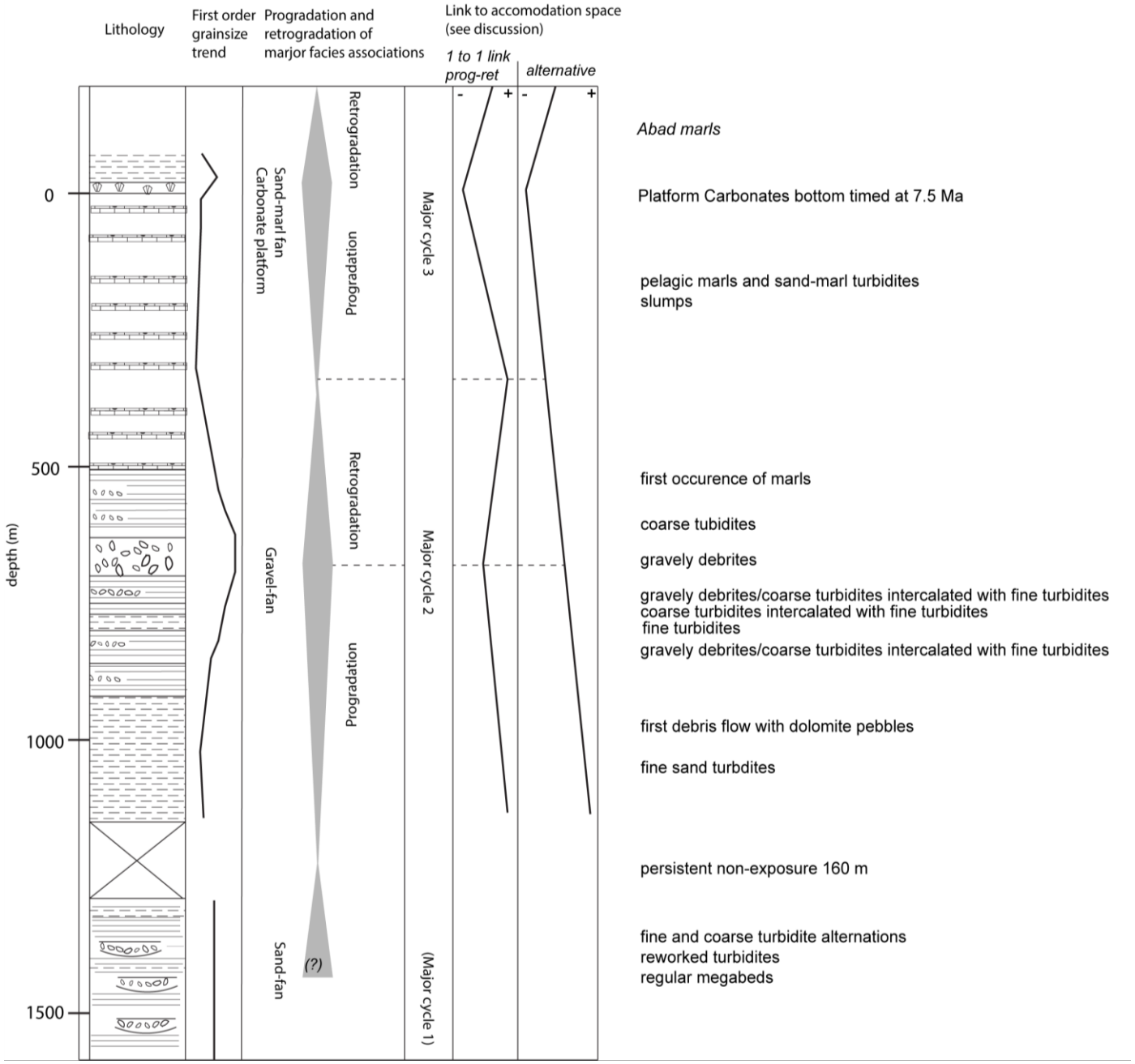


**Figure 21:** Summary of the large scale basinfill with the first order grainsize trend, the major cycles and progradation and retrogradation of facies. On the right the link between the progradation retrogradation of the facies and the evolution of accommodation space see discussion Ch. 10.3

# 10. Discussion

## 10.1 Validation of the section

Since only one high resolution cross-section was recorded some assumptions have to be made with regard to the stratigraphy. Because most turbidites are fine grained and sheet-like in character and the basin is very narrow (only 15 km from one side to the other), it is assumed that the individual flows are able to cover a sufficient large part of the basin so that autocyclic processes such as lobe switching do not play a major role. The facies that has to be regarded with lobe-switching are the gravely debrites which are prone to be less continuous laterally (*Shanmugam 2006*) and are therefore make the section more sensitive to autocyclic processes. The transitions between cycles are however gradual while a more abrupt transition would be expected if lobe switching played a large role.

## 10.2 Basin Age

If the sedimentation rates (1.25-2.25 m/kyr) for the sand-marl fan are extrapolated from the base of the platform carbonates at 7.5 downward this implies a younger base of the basin-fill than previously thought. The base of the 1600 m package of sediments in our section would be consequently dated at ~8.2-8.8Ma. This is significantly younger than the late Serravallian to lower Tortonian age (11-12Ma) for the red conglomerates which is still poorly constrained. The question hereby is whether the turbidites found near the NARF in our section are the deep water equivalent of the marine conglomerates towards the east of the basin or that these conglomerates are not exposed in our section but have remained at depth (*see do Couto 2014*). The latter model would mean that is stratigraphy missing and ~8.2-8.8 is not the initiation of sedimentation in the Sorbas Basin. However to arrive at 11 Ma the missing section would have to be roughly 2700-5000m which is highly unlikely given a recent gravimetric study (do Couto 2014) . The younger age of the basinfill if the sedimentation rates are a good estimation would consequently mean an even high subsidence rate than the one discussed below (10.3.1).

## 10.3 External controls on basin fill

The main external controls on a basinfill considered are Eustatic sea-level change, tectonics and sediment supply. We discuss here the ability of each of these controls to affect the accommodation and/or supply with respect to the environments in the Sorbas Basin.

### *10.3.1 Tectonics*

Tectonic subsidence in the Sorbas basin has been in the order of 1 km within a time interval of approximately 3.5 Ma derived from backstripping (Cloetingh et al 1992). This implicates an average subsidence rate of 0.3mm/yr. At these high rates subsidence is probably of major influence on the creation of accommodation space. Particularly in extensional detachments tectonic subsidence in the hangingwall is accompanied by exhumation in the footwall which is expected to have its implications on sediment supply (see below).

Tectonics can also have negative effect on the accommodation space through uplift by inversion. In our fault analysis however we concluded that the major inversion did not place in the Tortonian but at a later time.

*10.3.2 Sediment supply*

Sediment supply is a function of climate and regional geography. Climate influences precipitation controlling the run-off from the source area to the basin. The areas of highest sedimentation are those of periodical high precipitation alternating with dry periods (e.g. *van der Zwan 2002 and references therein*). The regional geography determines the catchment area and the gradient of this area is determined by the relief. During high tectonic activity the Sierra Alhamilla/Cabrera in the footwall will be exhumed rejuvenating the source area and possibly creating relief. This will has an increased effect on sediment supply.

*10.3.3 Eustatic sea level change*

Eustatic sea-level change could control the facies distribution by controlling the sedimentation on the shelf in the footwall. A sea-level rise would force back sedimentation on the shelf starving the basin while a sea-level fall would promote bypass of the shelf and supply to the basin. It is questionable whether eustasy was able to influence the Sorbas basin fill significantly. Firstly eustatic sea-level changes during the Tortonian fluctuated between +20 and -20 meter (e.g. Haq et al 1987, Miller 2005). In addition Blum and Womack (2009) pointed out that on narrow shelves the capability to store sediment is low and rivers often transverse the shelf depositing directly in the deep-water during both Lowstand and Highstand. Deep-water systems are consequently always supplied independently of Eustatic sea-level changes. A narrow shelf is envisaged for the depositional environments of the alluvial gravel fan and the early phase of the carbonate platform to sand-marl fan (figures 18 and 19). Therefore a model where sedimentation retreats to the shelf is unlikely in these settings. Taking into account these factors it is assumed that Eustatic sea-level did not play a major role in controlling the facies distribution during periods of high tectonic subsidence.

**10.4 Controls on Major cycles**

The transition from Major cycle 1 (sand-fan) to the progradation in the gravel facies in major cycle 2 (fig.21) was forced by a major change in source area caused by the emergence of the sierra Alhamilla/Cabrera probably caused by the continuing uplift of the footwall during extension. the Tectonic thus caused a rapid increase in supply (A'<S') forcing progradation. This in combination with the steep slope in the footwall formed by the controlling fault enables the transport of very coarse material an progradation of the submarine part. From the moment that the Sierras emerge they remain a source area by the continuing footwall uplift. The retrogradation of the gravel-fan facies (fig. 21) has been attributed to the filling of the basin leading to the building of a slope which is less steep than the slope formed by the controlling fault (fig. 19 Ch. 8.3.2).

This is an autogenic process although the filling itself is related to relatively *decreasing* accommodation space. Laying the link between the retrogradation of the gravel-fan facies and *increasing* accommodation

space (A'>S') might therefore be unjustified in this case. Alternatively one could interpret the whole sequence from the base of Major cycle 2 to the platform carbonates as 1 large prograding stack with decreasing accommodation space (fig. 21).

### 10.5 Controls on Intermediate cycles

*10.5.1 In the Sand fan (major cycle 1)*

While the sediment source is in the north we envisaged a model where sedimentation retreats to the shelf during periods where A'>S' on this shelf. Given the high subsidence rate compared to eustatic sea-level changes and the position of this shelf being in the hangingwall, this is likely a process controlled by tectonics. In addition the asymmetrical shape with a relatively short retrogradation and a relatively long progradation has been associated with alternating phases of high tectonic activity (subsidence) and relative tectonic quiescence (*e.g. Martins-Neto 2010, Davies 2003*). Phases of high tectonic subsidence lead to a rapid retrogradation, associated with the deposition of fine grained turbidites (fig. 22). are alternating with phases of tectonic quiescence and a long progradation (fig. 22). While the entire basin-fill only spans 3.5 Ma (or less), given their limited stratigraphic thickness the time in these cycles could be less than 200kyr or even less.

Another indicator of tectonic activity is the presence of the Megabeds indicates that the distribution of sediments is partly controlled by slope failure. This is likely the consequence of the tectonic activity creating earthquakes triggering The tectonics trigger coarse sand deposition from mass flows and at the same time cause subsidence so that a retrogradation occurs above the megabed (fig.22). In addition Megabeds might occur on their own (fig.20; Appendix A) occur surrounded by types 48, 38, 33 associated with high tectonic activity (subsidence) which is another indication for triggering by seismic activity.

*10.5.2 In the Gravel fan (major cycle 2)*

In Major cycle 2 (fig, 21), two intermediate cycles could be defined of 100-150 m (Appendix A). Again these cycles have an asymmetrical shape with a relatively short retrogradation and a relatively long progradation which has been associated with phases of tectonic subsidence (*e.g. Martins-Neto 2010, Davies 2003*). These phases of high tectonic activity also cause exhumation in the footwall rejuvenating the source area and creating relief so that after the initial rapid increase in accommodation space (A'>S') a rapid increase in supply will force a progradation (A'<S') (fig.23).

Alternatively, if the sedimentation rates remain similar to those calculated for the sand marl fan (1.25 - 2.25m/kyr) these cycles might be the expression of the 100kyr eccentricity cycle modulating smaller precession driven cycles (Appendix A; also see Postma 1993, Hüsing 2008). In this model the supply from the footwall would be directly controlled by climate. During wet periods with increased run-off related to precession minima (e.g. Rossignol-Strick 1983) supply to the basin is high whereas during dry periods the supply is low. This might be a better model as it is questionable whether the creation of accommodation space is really sufficient to cause retrogradation in the fan if it is assumed that the flows are always deposited downslope of the steep footwall slope. The 5 smaller cycles identified in the first intermediate cycle (Appendix A) would then be the 20kyr precession cycles.

*10.5.3 In the Carbonate platform to sand-marl fan (Major cycle 3)*

In major cycle 3 the intermediate cycles are possibly related to precession cycles indicated by the timing constraint (see Ch. 9.3.3). These cycles do not have the characteristic signature of short retrogradation followed by a long progradation (fig.20; Appendix A). Therefore we propose a model where climate controls the supply of sand to the basin and with that the alternation between turbiditic and carbonatic pelagic deposition (fig. 24). A similar model model has also been proposed by Garcia-Garcia et al. (2009) for the Late Tortonian sequence in the Gaudix basin, ~80 km North East of the Sorbas basin. They propose a model where during cool-wet periods the supply of sand is large, creating mainly sandy deposits while during cold-dry periods pelagic sedimentation dominates with only sporadic turbidity currents related to precession cycles. This is a likely scenario for the Sorbas basin as well (fig. 24).

Another model would be the formation of the shelf during the progradation of the platform carbonates into the basin (fig. 19). In this setting sea-level change by climate has a much larger effect while it can control the sedimentation to the deep-water (Ch. 10.3.3). For a better distinction between sea level and supply driven cycles however, also bio-stratigraphic data should be integrated but this is not yet available. Where both eustatic sea-level and sediment supply are controlled by climate, it can be concluded a shift from tectonically controlled to climate controlled Intermediate cycles occurs in the Sorbas Basin fill.

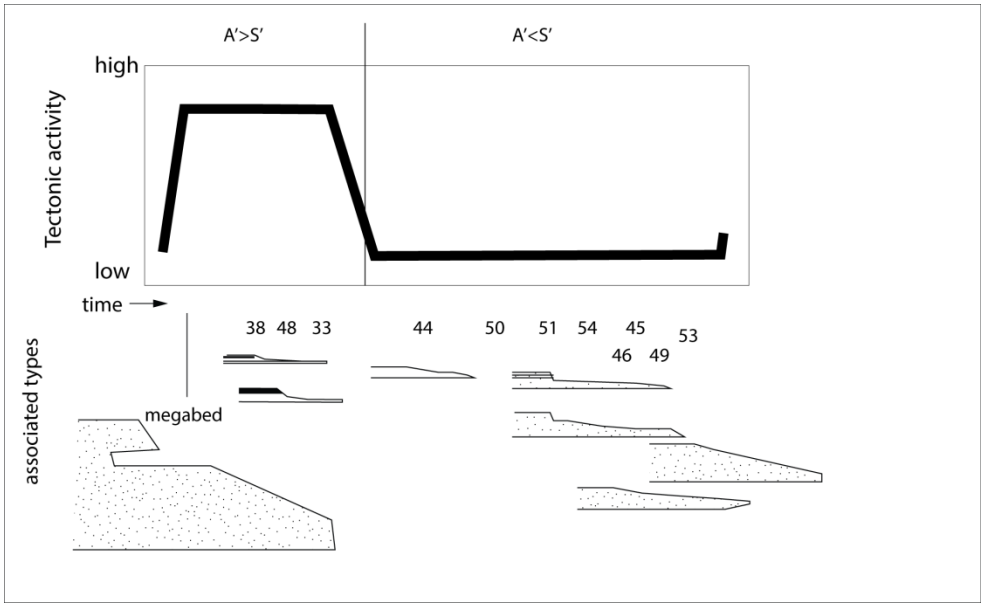


**Figure 22:** Envisaged correlation between Tectonic activity; progradation retrogradation and the related types in the Sand-fan (major cycle 1). The Megabeds can also occur surrounded by types 48, 38, 33 associated with high tectonic activity (subsidence) which is another indication for triggering by seismic activity Types are depicted as in the stratigraphic column (Appendix A).

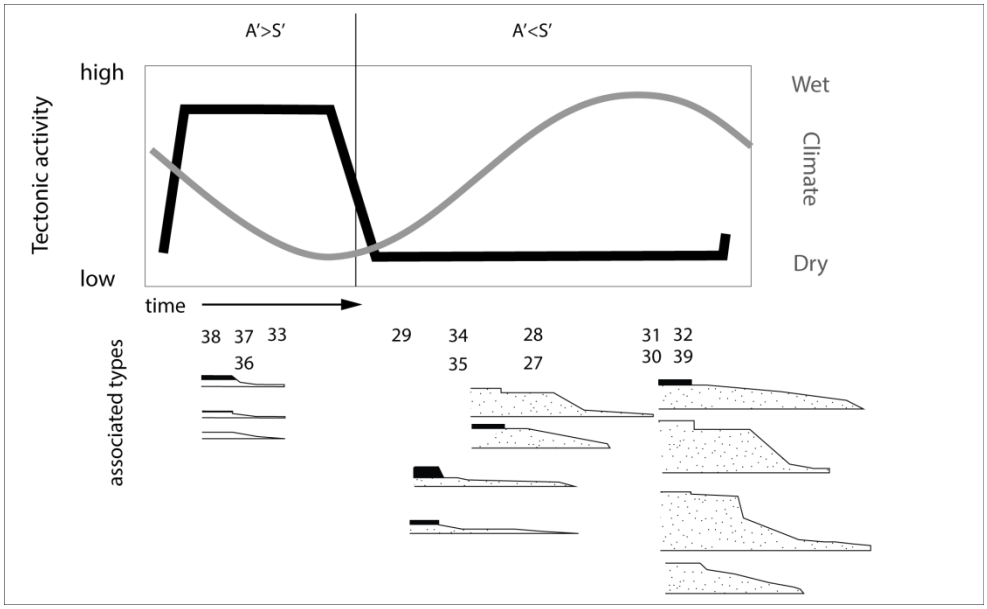


**Figure 23**: Envisaged correlation between tectonic activity or alternatively climate. Progradation retrogradation and the related types in the gravel-fan (major cycle 2) could be related to pulses of high subsidence or to precession forced alternating dry and wet periods. Types are depicted as in the stratigraphic column (Appendix A).

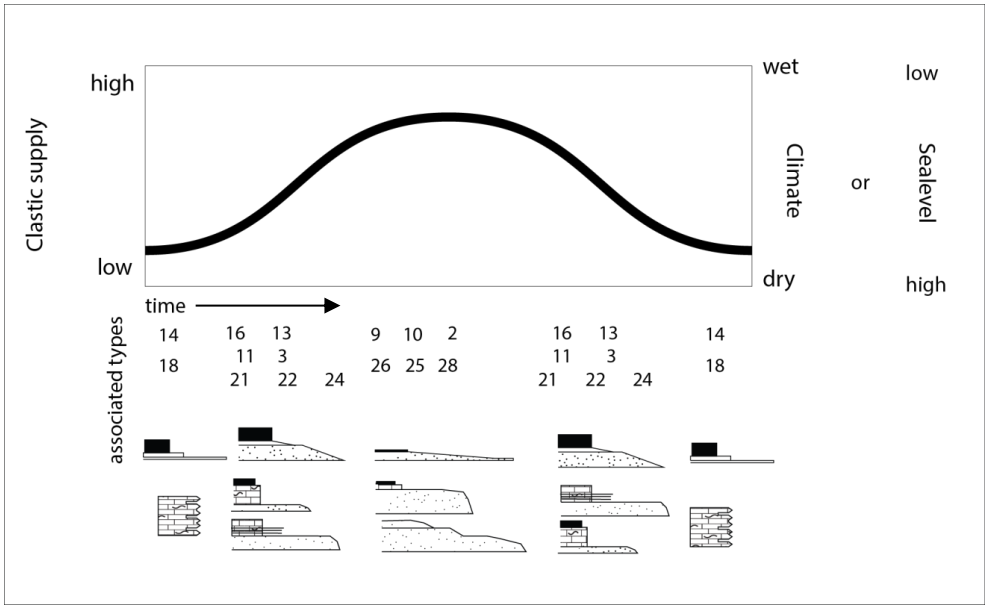


**Figure 24**: Envisaged correlation between the cyclic supply of clastic material and the deposited facies controlled by climate in the san-marlfan (major cycle 3). Climate could control supply by eustatic sea-level and could control directly the supply of clastic sediments to the basin resulting in a similar pattern of facies. Types are depicted as in the stratigraphic column (Appendix A).

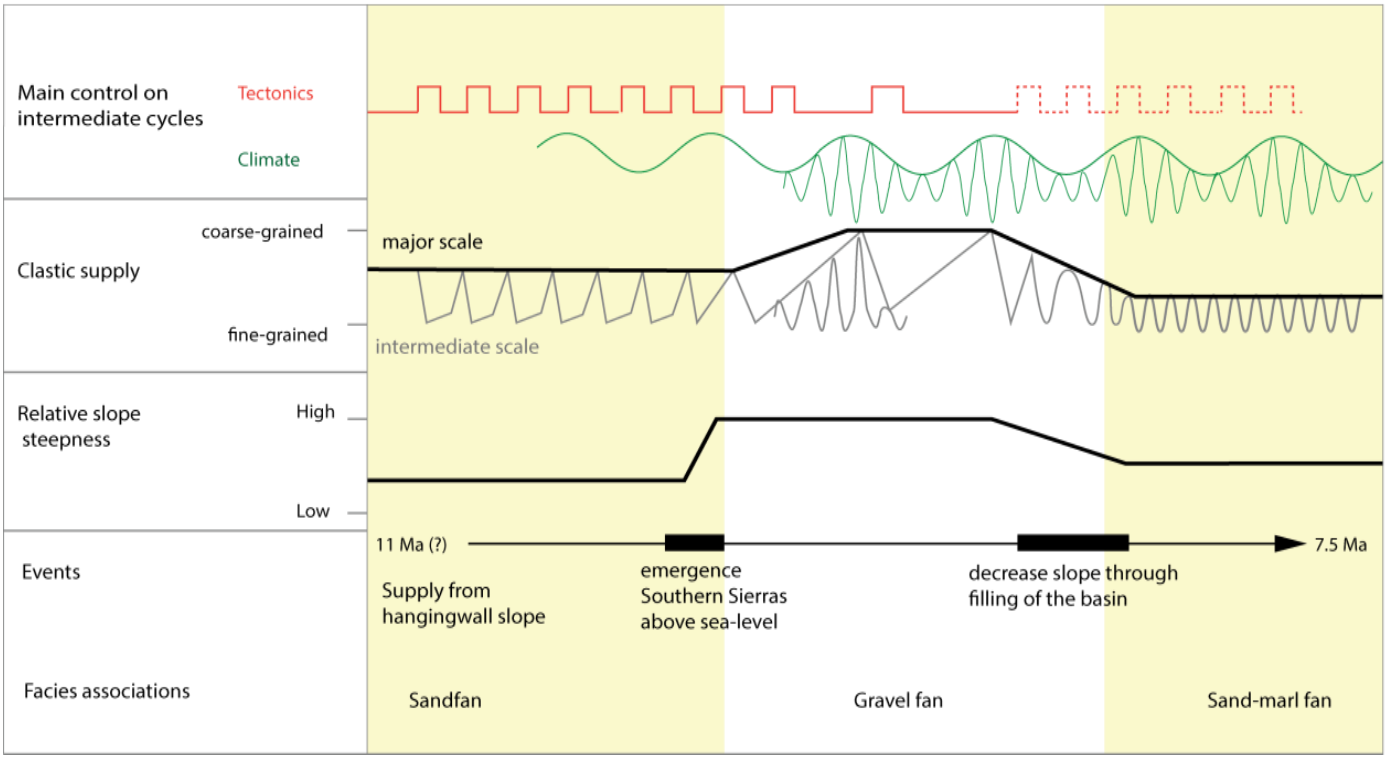


**Figure 25:** Controls on facies distribution throughout the life of the Sorbas basin. Tectonics with pulses of high activity was probably the main factor controlling intermediate cycles in the early phase with slope failure as an important depositional process. Climate with precession cycles modulated by 100kyr eccentricity (conceptual curve) is likely responsible for forcing of the intermediate cycles in the later phase when the supply came from the footwall. The large scale non-cyclical facies changes were caused by the emergence of the Southern Sierras and the filling of the basin.

---

## 11. Conclusions

*Implications for the Sorbas Basin*

The boundary between the turbidites and the carbonate platform deposits has been interpreted as a facies limit rather than an unconformity. The clinoform shape implicates that this boundary is diachronous as the timelines do not go horizontal. Given the direction of progradation this boundary is expected to be younging towards the West-Northwest.

Extension might have lasted longer than previously thought as syn-kinematic faulting has been witnessed up to and into the carbonate platform facies. It is therefore proposed that the inversion of the basin is not Late Tortonian but probably Upper Messinian. We speculate that the onset of inversion occurred in the Abad unit associated with progressive restriction of the basin (*e.g. Sierro 1999*) and continued throughout the Messinian eventually leading to the deposition of evaporitic gypsum which could not be correlated to eustatic sea-level changes (*Hodell 2004*).

The onset of sedimentation in the Sorbas Basin probably occurred Later in time. If the sedimentation-rates calculated are a good indication of the sedimentation rate throughout the basin fill this age would be around 9Ma instead of 11-12Ma. Better timing constraint on the Tortonian sequence is however a good objective for future studies.

*Implications for asymmetrical basins:*

Some factors that are inherent to asymmetrical extensional basins are strongly controlling the facies distribution at multiple scales in the Sorbas Basin and might be in some way applicable to other basins. These factors are: (1) high footwall exhumation, (2) high subsidence rates and (3) the asymmetrical basin geometry itself with a low inclined hangingwall slope and a steeply inclined footwall slope.

On a large scale (multiple 100s of meters) 2 major facies changes could be distinguished forced by these factors. The transition from the sand-fan facies to the gravel-fan facies was caused by the emergence of the southern Sierras (1) establishing a source in the south (fig. 25). The combination of high sediment availability in a very proximal area (1) and, importantly a high slope in the footwall (3) causes the deposition of the coarsest facies (fig.25).

The transition from the gravel-fan facies to the sand-marl facies was caused by a change in the steep footwall slope. The inclination of the steep footwall slope (3, 1) decreases as the basin fills up (fig. 25). In a deep-water setting with dominantly gravity flows, this might lead to a fining upwards (Ch. 10.3). This is expressed in the Sorbas Basin in the retrogradation of the gravel-facies of coarse turbidites and debris flows which is replaced by an environment dominated by fine-grained flows and pelagic settling (fig. 25). This is contrary to the general model of coarsening upwards towards the end of basin-fill related to the decrease in accommodation space relative to supply.

On Intermediate scale (20-150m) tectonics but more prominently climate plays a large role controlling directly sediment supply to the basin. In the sand fan facies association tectonics controls distribution of coarse material by limiting sedimentation to the shelf during pulses of high subsidence and by inducing slope-failure.

In the gravel fan association a model of tectonic control is less likely as there is no shelf and it is questionable whether the generation of accommodation space in the basin is relevant for gravity driven flows that bypass the steep footwall slope and are deposited in the depocenter. The cycles found in this association are likely precession controlled where supply is fluctuating between wet and dry periods. The 100kyr eccentricity cycle modulating precession is a likely cause for the larger 100m trends (fig. 25).

A similar precession controlled system is envisaged for the sand-marl fan. During dry periods of reduced run-off little siliciclastic material is supplied to the fan while pelagic sedimentation dominates. During wet periods of high run-of the fan is nourished with siliciclastic material from the footwall. Note that deposition during this phase is less coarse because of the lower slope (fig.25).

The smallest scale cycles were Minor cycles (meter scale) observed along intrabasinal syn-depositional normal faults related to the extension. Activity on these faults is likely related to activity on the main controlling fault causing a short-lived retrogradation at this scale.

**Appendix A**

Includes the high resolution stratigraphic column. Indicated are transgression regression trends with the corresponding types. Grainsizes of types are indicated by their extend on the x-axis and lithology is; black clay, white sand hashed are marls. Also indicated are the moments of faulting (**F**) and positions of megabeds.

**Appendix B**

Includes descriptions of the lithological types identified in the field. Indicated are the sizes, the composition, grainsize and internal structures.

## References


Augier, R., L. Jolivet, D. Do Couto et al. (2013), From ductile to brittle, late- to post-orogenic evolution of the Betic Cordillera: Structural insights from the northeastern Internal Zones. Bulletin de la Societe Geologique de France 184(4-5), pp.405-425.

Augier, R., L. Jolivet & C. Robin. (2005), Late orogenic doming in the eastern Betic Cordilleras: Final exhumation of the Nevado-Filabride complex and its relation to basin genesis. Tectonics 24(4), pp.1-19.

Baggley, K.A. (2000), The late tortonian-early messinian foraminiferal record of the abad member (turre formation), Sorbas Basin, Almería, south-east Spain. Palaeontology 43(6), pp.1069-1112.

Blum, M.D. & J. Hattier-Womack. (2009), Climate change, sea-level change, and fluvial sediment supply to deepwater depositional systems. External Controls on Deepwater Depositional Systems: SEPM, Special Publication 92, pp.15-39.

Braga, J.C., J.M. Martín, C. Betzler et al. (2006), Models of temperate carbonate deposition in Neogene basins in SE Spain: A synthesis. Geological Society, London, Special Publications 255(1), pp.121-135.

Braga, J.C., J.M. Martín & C. Quesada. (2003), Patterns and average rates of Late Neogene- recent uplift of the Betic Cordillera, SE Spain. Geomorphology 50(1-3), pp.3-26.

Byerlee, J. (1978), Friction of rocks. Pure and Applied Geophysics 116(4-5), pp.615-626.

Catuneanu, O. (2006). Principles of sequence stratigraphyElsevier.

Cloetingh, S., P. Van der Beek, D. Van Rees et al. (1992), Flexural interaction and the dynamics of neogene extensional basin formation in the Alboran-Betic region. Geo-Marine Letters 12(2-3), pp.66-75.

Davies, S.J. & M.R. Gibling. (2003), Architecture of coastal and alluvial deposits in an extensional basin: The Carboniferous joggins formation of eastern Canada. Sedimentology 50(3), pp.415-439.

De Boer, P.L. & D.G. Smith. (1994), Orbital forcing and cyclic sequences. Orbital forcing and cyclic sequences, pp.1-14.

Do Couto, D., C. Gumiaux, R. Augier et al. (2014), Tectonic inversion of an asymmetric graben: Insights from a combined field and gravity survey in the Sorbas Basin. Tectonics 33

Embry, A. & E. Johannessen. (1992), TR sequence stratigraphy, facies analysis and reservoir distribution in the uppermost Triassic-Lower Jurassic succession, western Sverdrup basin, Arctic Canada. Arctic geology and petroleum potential 2, pp.121-146.

Fabbi, S. & M. Santantonio. (2012), Footwall progradation in syn-rift carbonate platform-slope systems (early jurassic, northern Apennines, Italy). Sedimentary Geology 281(0), pp.21-34. DOI:

Fernando, G.-., J.M. Soria, C. Viseras et al. (2009), High-frequency rhythmicity in a mixed siliciclastic-carbonate shelf (late Miocene, Guadix basin, Spain): A model of interplay between climatic oscillations, subsidence, and sediment dispersal. Journal of Sedimentary Research 79(5-6), pp.302-315.

Fortuin, A. & W. Krijgsman. (2003), The Messinian of the Nijar basin (SE Spain): Sedimentation, depositional environments and paleogeographic evolution. Sedimentary Geology 160(1), pp.213-242.

García-García, F., Soria, J. M., Viseras, C., & Fernández, J. (2009). High-Frequency Rhythmicity in a Mixed Siliciclastic–Carbonate Shelf (Late Miocene, Guadix Basin, Spain): A Model of Interplay Between Climatic Oscillations, Subsidence, and Sediment Dispersal. *Journal of Sedimentary Research*, *79*(5), 302-315.

Gawthorpe, R.L., A.J. Fraser & R.E.L. Collier. (1994), Sequence stratigraphy in active extensional basins: Implications for the interpretation of ancient basin-fills. Marine and Petroleum Geology 11(6), pp.642-658.

Goldfinger, C., C.H. Nelson & J.E. Johnson. (2003), Holocene earthquake records from the Cascadia subduction zone and northern San Andreas fault based on precise dating of offshore turbidites. Annual Review of Earth and Planetary Sciences 31(1), pp.555-577.

Gorsline, D., T. De Diego & E. Nava-Sanchez. (2000), Seismically triggered turbidites in small margin basins: Alfonso basin, western Gulf of California and Santa Monica basin, California borderland. Sedimentary Geology 135(1), pp.21-35.

Haq, B.U., J. Hardenbol & P.R. Vail. (1987), Chronology of fluctuating sea levels since the Triassic. Science (New York, N.Y.) 235(4793), pp.1156-1167.

Haughton, P. (2001), Contained turbidites used to track sea bed deformation and basin migration, Sorbas basin, south-east Spain. Basin Research 13(2), pp.117-139.

Haughton, P. (1994), Deposits of deflected and ponded turbidity currents, Sorbas basin, southeast Spain. Journal of Sedimentary Research A: Sedimentary Petrology & Processes 64 A(2), pp.233-246.

Haughton, P. (2000), Evolving turbidite systems on a deforming basin floor, Tabernas, SE Spain. Sedimentology 47(3), pp.497-518.

Hilgen, F., W. Krijgsman, C. Langereis et al. (1995), Extending the astronomical (polarity) time scale into the Miocene. Earth and Planetary Science Letters 136(3), pp.495-510.

Hodell, D.A., J.H. Curtis, F.J. Sierro et al. (2001), Correlation of late Miocene to early Pliocene sequences between the Mediterranean and North Atlantic. Paleoceanography 16(2), pp.164-178.

Hüsing, S. (2008), Astrochronology of the Mediterranean Miocene: Linking palaeoenvironmental changes to gateway dynamics. Geologica Ultraiectina 295

James, N. (1997), The cool-water carbonate depositional realm. SPECIAL PUBLICATION-SEPM 56, pp.1-22.

Johnson, C., N. Harbury & A.J. Hurford. (1997), The role of extension in the Miocene denudation of the Nevado-Filábride complex, Betic Cordillera (SE Spain). Tectonics 16(2), pp.189-204.

Johnson, J. & M. Murphy. (1984), Time-rock model for Siluro-Devonian continental shelf, western United States. Geological Society of America Bulletin 95(11), pp.1349-1359.

Kleverlaan, K. (1987), Gordo megabed: A possible seismite in a Tortonian submarine fan, Tabernas Basin, province almeria, southeast Spain. Sedimentary Geology 51(3–4), pp.165-180.

Krijgsman, W., A.R. Fortuin, F.J. Hilgen et al. (2001), Astrochronology for the Messinian Sorbas Basin (SE Spain) and orbital (precessional) forcing for evaporite cyclicity. Sedimentary Geology 140(1-2), pp.43-60.

Krijgsman, W., A.R. Fortuin, F.J. Hilgen et al. (2001), Astrochronology for the messinian Sorbas Basin (SE Spain) and orbital (precessional) forcing for evaporite cyclicity. Sedimentary Geology 140(1-2), pp.43-60.

Martin, J. & J. BRAG. (1996), S9 tectonic signals in the messinian stratigraphy of the Sorbas Basin (Almeria, SE Spain). Tertiary basins of Spain: the stratigraphic record of crustal kinematics(6), pp.387.

Martín, J.M. & J.C. Braga. (1990), Arrecifes messinienses de Almería. tipologías de crecimiento, posición estratigráfica y relación con las evaporitas.

Martín, J.M., J.C. Braga & r. riding. (1997), Late Miocene halimeda alga-microbial segment reefs in the marginal Mediterranean Sorbas Basin, Spain. Sedimentology 44(3), pp.441-456.
Martín, J. & J.C. Braga. (1994), Messinian events in the Sorbas Basin in southeastern Spain and their implications in the recent history of the Mediterranean. Sedimentary Geology 90(3-4), pp.257-268.
Martínez-Martínez, J.M. & J.M. Azañón. (1997), Mode of extensional tectonics in the southeastern Betics (SE Spain): Implications for the tectonic evolution of the peri-Alborán orogenic system. Tectonics 16(2), pp.205-225.
Martins-Neto, M.A. & O. Catuneanu. (2010), Rift sequence stratigraphy. Marine and Petroleum Geology 27(1), pp.247-253.
Miller, K.G., M.A. Kominz, J.V. Browning et al. (2005), The Phanerozoic record of global sea-level change. Science 310(5752), pp.1293-1298.
Mitchum Jr., R.M. & J.C. Van Wagoner. (1991), High-frequency sequences and their stacking patterns: Sequence-stratigraphic evidence of high-frequency eustatic cycles. Sedimentary Geology 70(2-4), pp.131-"147,153-160".
Montenat, C. & P. Ott D'Estevou. (1999), The diversity of Late Neogene sedimentary basins generated by wrench faulting in the eastern Betic Cordillera, SE Spain. Journal of Petroleum Geology 22(1), pp.61-80.
Mutti, E. & F. Ricci Lucchi. (1972), Le torbiditi dell'Appennino settentrionale: Introduzione all'analisi di facies. Mem.Soc.Geol.Ital 11(2), pp.161-199.
Pereira, R. & T.M. Alves. (2012), Tectono-stratigraphic signature of multiphased rifting on divergent margins (deep-offshore southwest Iberia, North Atlantic). Tectonics 31(4)
Platt, J., S. Kelley, A. Carter et al. (2005), Timing of tectonic events in the Alpujárride complex, Betic Cordillera, southern Spain. Journal of the Geological Society 162(3), pp.451-462.
Postma, G., Hilgen, F. J., & Zachariasse, W. J. (1993). Precession-punctuated growth of a late Miocene submarine-fan lobe on Gavdos (Greece). Terra Nova, 5(5), 438-444.
Puga-Bernabéu, Á., J.C. Braga & J.M. Martín. (2007), High-frequency cycles in upper-Miocene ramp-temperate carbonates (Sorbas Basin, SE Spain). Facies 53(3), pp.329-345.
Reading, H.G. & M. Richards. (1994), Turbidite systems in deep-water basin margins classified by grain size and feeder system. American Association of Petroleum Geologists Bulletin 78(5), pp.792-822.
Riding, R., J. Braga & J. Martın. (2000), Late Miocene Mediterranean desiccation: Topography and significance of the 'Salinity crisis' erosion surface on-land in southeast Spain: Reply. Sedimentary Geology 133(3), pp.175-184.
Riding, R., J.M. Martin & J.C. Braga. (1991), Coral-stromatolite reef framework, upper Miocene, Almería, Spain. Sedimentology 38(5), pp.799-818.
Rodríguez-Fernández, J. & C. Sanz de Galdeano. (2006), Late orogenic intramontane basin development: The Granada Basin, Betics (southern Spain). Basin Research 18(1), pp.85-102. DOI: 10.1111/j.1365-2117.2006.00284.x
Rodríguez-Fernández, J., A. Azor & J. Miguel Azañón. (2011). The betic intramontane basins (SE Spain): Stratigraphy, subsidence, and tectonic history. Tectonics of sedimentary basins, pp. 461-479John Wiley & Sons, Ltd. DOI:10.1002/9781444347166.ch23.
Rossignol-Strick, M. (1983). African monsoons, an immediate climate response to orbital insolation. Nature, 304(5921), 46-49.
Sánchez-Almazo, I.M., B. Spiro, J.C. Braga et al. (2001), Constraints of stable isotope signatures on the depositional palaeoenvironments of upper Miocene reef and temperate carbonates in the Sorbas Basin, SE Spain. Palaeogeography, Palaeoclimatology, Palaeoecology 175(1-4), pp.153-172.
Schlager, W. (1993), Accommodation and supply-a dual control on stratigraphic sequences. Sedimentary Geology 86(1-2), pp.111-136.
Shanmugam. (2006). Deep-water processes and facies models
Sierro, F.J., J.A. Flores, I. Zamarreño et al. (1999), Messinian pre-evaporite sapropels and precession-induced oscillations in western Mediterranean climate. Marine Geology 153(1-4), pp.137-146.
Song, T. & P.A. Cawood. (2001), Effects of subsidiary faults on the geometric construction of listric normal fault systems. AAPG Bulletin 85(2), pp.221-232.

Stapel, G., R. Moeys & C. Biermann. (1996), Neogene evolution of the Sorbas Basin (SE Spain) determined by paleostress analysis. Tectonophysics 255(3), pp.291-305.
Van der Zwan, C.J. (2002), The impact of milankovitch-scale climatic forcing on sediment supply. Sedimentary Geology 147(3–4), pp.271-294.
Vázquez, M., A. Jabaloy, L. Barbero et al. (2011), Deciphering tectonic-and erosion-driven exhumation of the Nevado–Filábride complex (betic cordillera, southern Spain) by low temperature thermochronology. Terra Nova 23(4), pp.257-263.
Vissers, R., J. Platt & D.v.d. Wal. (1995), Late orogenic extension of the Betic Cordillera and the Alboran domain: A lithospheric view. Tectonics 14(4), pp.786-803.
Weijermars, R., T.B. Roep, V. Van Den Eeckhout et al. (1985), Uplift history of a betic fold nappe inferred from Neogene- Quaternary sedimentation and tectonics (in the Sierra Alhamilla and Almeria, Sorbas and Tabernas Basins of the Betic Cordilleras, SE Spain. Geologie en Mijnbouw 64(4), pp.397-411.
Wernicke, B. & G.J. Axen. (1988), On the role of isostasy in the evolution of normal fault systems. Geology 16(9), pp.848-851.
Winter, d.N.J. & J.D. Hartman. (unpublished), An astronomically tuned age for the base of the Azagador member in the Sorbas Basin and relations to the Tabernas basin, Spain.
Withjack, M.O., Q.T. Islam & P.R. La Pointe. (1995), Normal faults and their hanging-wall deformation: An experimental study. American Association of Petroleum Geologists Bulletin 79(1), pp.1-18.